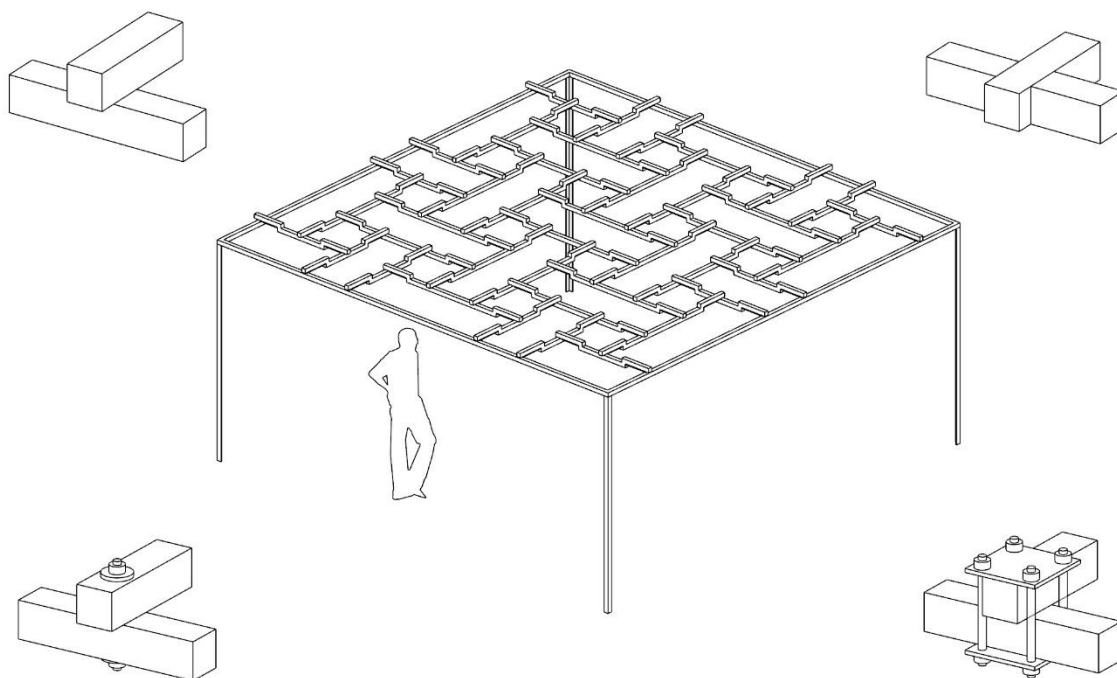




**CHALMERS**  
UNIVERSITY OF TECHNOLOGY



# Connections in Timber Reciprocal Frames

Master's Thesis in the Master's Programme Structural Engineering and Building Technology

JOEL GUSTAFSSON

---

Department of Civil and Environmental Engineering  
*Division of Structural Engineering*  
*Steel and Timber Structures*  
CHALMERS UNIVERSITY OF TECHNOLOGY  
Gothenburg, Sweden 2016  
Master's Thesis BOMX02-16-69



MASTER'S THESIS BOMX02-16-69

# Connections in Timber Reciprocal Frames

*Master's Thesis in the Master's Programme Structural Engineering and Building Technology*

JOEL GUSTAFSSON

Department of Civil and Environmental Engineering

*Division of Structural Engineering*

*Steel and Timber Structures*

CHALMERS UNIVERSITY OF TECHNOLOGY

Göteborg, Sweden 2016



## **Connections in Timber Reciprocal Frames**

*Master's Thesis in the Master's Programme Structural Engineering and Building Technology*

JOEL GUSTAFSSON

© JOEL GUSTAFSSON, 2016

Examensarbete BOMX02-16-69/ Institutionen för bygg- och miljöteknik,  
Chalmers tekniska högskola 2016

Department of Civil and Environmental Engineering  
Division of Structural Engineering  
Steel and Timber Structures  
Chalmers University of Technology  
SE-412 96 Göteborg  
Sweden  
Telephone: + 46 (0)31-772 1000

Cover:

The cover picture shows a reciprocal frame structure and the connection types that are treated in this thesis.

Department of Civil and Environmental Engineering. Göteborg, Sweden, 2016



# Connections in Timber Reciprocal Frames

*Master's thesis in the Master's Programme Structural Engineering and Building Technology*

JOEL GUSTAFSSON

Department of Civil and Environmental Engineering  
Division of Structural Engineering  
Steel and Timber Structures  
Chalmers University of Technology

## ABSTRACT

The timber reciprocal frame is a very old type of structure, with certainty used as early as in the thirteenth century. Its fundamental principle is that a number of beam elements support each other without structural hierarchy, making it possible to span a larger distance than what one individual element could. In a contemporary context, reciprocal frames have gained attention for a number of reasons, such as to increase use of locally produced wood and to ease assembly, disassembly and reuse of elements.

Not so much of the research on reciprocal frames has investigated the connections in the structure and what impact they have on the overall structural behaviour. Hence, the main purpose of this thesis was to evaluate a number of connection types and to assess their influence on timber reciprocal frames.

When evaluating the connection types, the main objective was to assess how they influence the reciprocal frame in terms of production, assembly/disassembly, appearance and structural behaviour. Furthermore, the aim was to carry out a more detailed connection stiffness analysis and compare two connection types, one using notches and one with elements simply put on each other, a so called superposition connection. For the notched connection type, a viable structural design according to Eurocode 5 has been calculated.

After calculating the translational and rotational stiffness, it was used as input for a finite element model created in Karamba, an analysis tool available for the Rhinoceros plug-in Grasshopper. One of the connection types was also realized in a full scale structure which was tested for deflection and failure load.

The structural calculations showed that there are differences between how a notched connection and a superposition connection influence a certain reciprocal frame structure. The superposition connection resulted in higher maximum deflection, bending moment and shear force. On the other hand it generates no torsional moment in the elements, which the notched connection does.

As a conclusion, the choice of connection type has influence on all the investigated indicators, including the structural behaviour. Hence, reciprocal frames are no exception from the general rule that connections play a vital role for all aspects of designing a structure.

Key words: Reciprocal frame, Connections, FEM, Timber engineering, Rotational stiffness, Translational stiffness, Karamba.

# Anslutningar i reciproka träkonstruktioner

Examensarbete inom masterprogrammet Structural Engineering and Building Technology

JOEL GUSTAFSSON

Institutionen för bygg- och miljöteknik  
Avdelningen för Konstruktionsteknik  
Stål- och träbyggnad  
Chalmers tekniska högskola

## SAMMANFATTNING

Reciproka träkonstruktioner är en mycket gammal konstruktionstyp som med säkerhet kan sägas ha använts sedan tolvhundratalet. Dess grundläggande princip är att ett antal balkar ömsesidigt bär upp varandra utan inbördes hierarki, vilket gör det möjligt att överbrygga ett längre spann än vad en enskild balk skulle klara av. Idag har reciproka konstruktioner uppmärksammats av ett antal olika anledningar, tex som ett sätt att använda lokalproducerat trä och förenkla montering, demontering och återanvändning av de bärande elementen.

Inte så stor del av forskningen på reciproka konstruktioner har undersökt anslutningarna i strukturen och vilken påverkan de har på konstruktionens övergripande beteende. Därför är huvudsyftet med detta examensarbete att utvärdera ett antal anslutningstyper och bedöma deras påverkan på reciproka träkonstruktioner.

I en inledande och mer generell bedömning var huvudmålet att ta reda på kopplingarnas inflytande på reciproka konstruktioner i form av produktion, montering/demontering, utseende och beteende hos konstruktionen. Vidare var målet att utföra en mer detaljerad styrhetsanalys och jämföra två anslutningstyper, en med urtag och en utan urtag. För den kopplingstypen med urtag, en överlapsfog, har också en genomförbar struktur tagits fram enligt Eurocode 5.

Efter att styrheterna för translation och rotation beräknats användes dessa värden som indata i en finit elementmodell i Karamba, ett analysverktyg för Rhinoceros plug-in Grasshopper. En av kopplingstyperna byggdes också i full skala i en konstruktion som testades för nedböjning och brottlast.

Beräkningarna visade att det finns skillnader i hur en överlapsfog och en koppling utan urtag påverkar en specifik reciprok konstruktion. Anslutningen utan urtag ger högre maximal nedböjning, böjande moment och tvärkraft. Å andra sidan skapar den inget vridmoment i balkarna, vilket överlapsfogen gör.

Slutsatsen är att valet av anslutningstyp påverkar varje undersökt indikator, inklusive konstruktionens beteende. Således är reciproka konstruktioner inget undantag från den allmänna regeln att kopplingarna spelar en betydande roll för alla aspekter vid framtagandet av en struktur.

Nyckelord: Reciproka konstruktioner, Anslutningar, FEM, Träkonstruktion, Rotationsstyrhet, Translationsstyrhet, Karamba.

# Contents

ABSTRACT	I
SAMMANFATTNING	II
CONTENTS	III
PREFACE	VI
NOTATIONS	VII
1 INTRODUCTION	1
1.1 Background	1
1.2 Aim and objective	2
1.2.1 Aim	2
1.2.2 Objective	2
1.3 Limitations	3
1.4 Method	3
2 HISTORICAL BACKGROUND	4
2.1 Early use of reciprocity	4
2.2 Applications in Asia	4
2.3 Medieval and later structures in Europe	5
2.4 Scientific research in the twentieth century	6
2.5 Contemporary examples	7
3 ELEMENTS AND COMPOSITIONS	10
3.1 Fundamental parameters	10
3.2 Elongated elements	10
3.2.1 Rods	10
3.2.2 Panels	11
3.2.3 Blocks	11
3.3 Plate elements	12
3.4 Ring elements	12
3.5 Combinations and alterations	13
3.6 Compositions	13
3.6.1 Flat compositions	13
3.6.2 Curved compositions	14
4 CONNECTION TYPES	15
4.1 Superposition	15
4.1.1 Pure superposition	15

4.1.2	Superposition with wedges	15
4.1.3	Production	15
4.1.4	Assembly, disassembly and reuse	16
4.1.5	Appearance	16
4.1.6	Structural properties	17
4.1.7	Built example	17
4.2	Couplers	17
4.2.1	Lashing	18
4.2.2	Contractile clamps	18
4.2.3	Joist hangers	18
4.2.4	Production	18
4.2.5	Assembly, disassembly and reuse	19
4.2.6	Appearance	19
4.2.7	Structural properties	19
4.2.8	Built example	20
4.3	Dowels and plates	21
4.3.1	Pure dowels	21
4.3.2	Nails and screws	22
4.3.3	Bolts	22
4.3.4	Plates	22
4.3.5	Glued-in rods	22
4.3.6	Production	23
4.3.7	Assembly, disassembly and reuse	23
4.3.8	Appearance	23
4.3.9	Structural properties	24
4.3.10	Built example	24
4.4	Notches	25
4.4.1	Half lap joints	25
4.4.2	Mortise and Tenon joints	26
4.4.3	Production	26
4.4.4	Assembly, disassembly and reuse	26
4.4.5	Appearance	26
4.4.6	Structural properties	27
4.4.7	Built example	27
4.5	Summary of evaluation	29
5	CONNECTION ANALYSIS	30
5.1	Context	30
5.2	Superposition connection	31
5.2.1	Stiffness analysis	31
5.3	Notched connection	33
5.3.1	Stiffness analysis	33
5.4	Global influence	38
5.4.1	The Karamba model	38
5.4.2	Results	45

<b>6 STRUCTURAL DESIGN</b>	49
6.1 Context and indata	49
6.2 Design procedure	49
6.2.1 Loads	50
6.2.2 Achieving deflection requirement	51
6.2.3 Design moments and forces	52
6.2.4 Check of capacities	52
6.2.5 Final design	55
<b>7 PHYSICAL MODEL</b>	56
7.1 Material	56
7.2 Production of notches	57
7.3 Assembly	58
7.4 SLS load test	60
7.4.1 Test setup	61
7.4.2 Results	62
7.5 Failure load test	63
7.5.1 Test setup	63
7.5.2 Results	64
<b>8 DISCUSSION</b>	68
8.1 Connection types	68
8.2 Connection analysis	68
8.3 Structural design	69
8.4 Physical model	69
<b>9 CONCLUSION</b>	71
9.1 Background	71
9.2 Evaluation	71
9.3 Design/Analysis	72
9.4 Physical model	73
<b>10 REFERENCES</b>	74
10.1 Literature	74
10.2 Web	75
10.3 Images	75

## Preface

This thesis was carried out at the Division of Structural Engineering, Steel and Timber Structures, at Chalmers University of Technology between January and May 2016. It was my degree project within the master's programme Structural Engineering and Building Technology and I would like to thank the following for their participation and support along the way:

Reza Haghani, Examiner, for very valuable supervision, especially with regard to connection stiffness analysis and finite element modelling.

Olga Popovic Larsen (KADK, Copenhagen), Supervisor, for important guidance on reciprocal frames, key suggestions and for overseeing the process and keeping me on the right track.

Jens Larsen (Arup, Copenhagen), Supervisor, for verification and input on the structural calculations.

Sebastian Almfeldt, Research Engineer, for all his help during the testing of the physical model.

Peter Lindblom and Tabita Nilsson, Heads of the Architecture Workshop, for advice on how to cut the beams in a good way.

Göteborg May 2016

Joel Gustafsson

# Notations

## Roman upper case letters

$A$	Cross section area
$C_t$	Translational stiffness
$C_r$	Rotational stiffness
$E$	Modulus of elasticity
$E_{0,mean}$	Elastic modulus parallel to the grain
$F$	Compression force
$G_{mean}$	Shear modulus
$G$	Permanent load
$I$	Moment of inertia
$J$	Polar moment of inertia
$L$	Length of spring
$M_x$	Bending moment around the x-axis
$M_{Rd}$	Design bending moment capacity
$M_{Ed}$	Design bending moment load effect
$T_{Rd}$	Design torsional moment capacity
$T_{Ed}$	Design torsional moment load effect
$V_{Rd}$	Design shear force capacity
$V_{Ed}$	Design shear force load effect

## Roman lower case letters

$d$	Lever arm of compression force
$f_k$	Characteristic strength
$f_d$	Design strength
$k$	Translational stiffness
$k_{cr}$	Decreasing factor with regard to cracks
$k_h$	Increasing factor with regard to cross section height
$k_{mod}$	Decreasing factor with regard to load duration
$k_{shape}$	Increasing factor with regard to cross section size
$k_v$	Decreasing factor with regard to notch
$r$	Radius of cross section
$w$	Deflection

## Greek letters

$\gamma$	Partial factor
$\delta$	Displacement
$\theta$	Rotation angle



# 1 Introduction

## 1.1 Background

Reciprocal frame (RF) structures can be defined as a composition of at least three load bearing elements which are mutually supported and interlocked. There is no structural hierarchy in the system, i.e. no classification of primary, secondary beams etc. and the elements can form either a flat or curved three dimensional frame system. In linguistics a “reciprocal construction” can mark a relationship between two nouns in a sentence. For example the sentence “Emil and Emilia helps each other” tells us that Emil helps Emilia and Emilia helps Emil. That is a good description of how a RF structure works: An element is supported by one element and supports another at the same time. By collaborating in this way, the beams can span a longer distance together than what they can do alone.

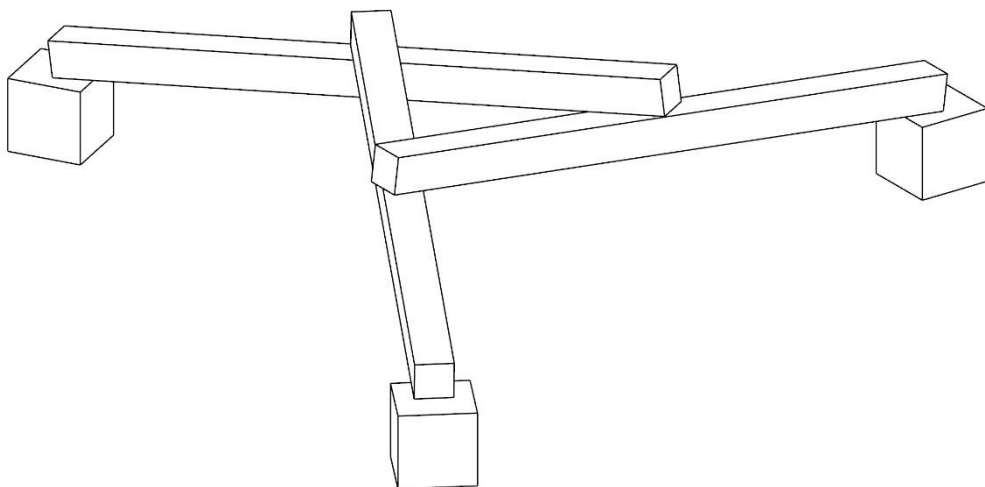


*Figure 1.1 A simple reciprocal frame with three elements.*

This structural scheme has with certainty been used since the thirteenth century (Pugnale & Sassone 2014) when it was implemented for spiral structures in Buddhist temples but there are also structures from earlier times with similar properties to RFs, such as the Indian tepee. In Western medieval buildings, RFs were used in floor constructions as a solution to lack of long timber members and Leonardo da Vinci made sketches of RF bridges in the fifteenth century.

In a contemporary context, RF structures have got attention as a way of using short members to span large distances. This makes it possible to use timber that is currently considered low grade. For example, trees grown near the construction site, that are perhaps too short to span the desired distance alone but sufficient in a RF formation, can then be used to a larger extent and thus reducing the transportation need in a sustainable way. The short elements are easy to handle and the need for heavy machinery on site can be limited. In RFs only two elements meet in a node and this allows for simple connections which are easy to assemble and disassemble. Thanks to its suitability for reuse, RFs have recently been used for temporary exhibition

pavilions and roof structures at archaeological excavation sites. RFs are also particularly suitable for excavation sites where the ground conditions are not entirely known thanks to their low sensibility to settlements (Gelez, Aubry & Vaudeville, 2011). Other possible contexts are emergency shelters and temporary bridges needed after natural disasters. In these scenarios the access of tools, machinery and craftsmen skill might be limited which make the RF structures a suitable alternative.

As for all structural systems, the design of connections has a significant influence on the structural behaviour of a RF as well as the assembly, disassembly and potential for reuse of its elements. Despite this importance, to date, only little research with regard to connections in RF structures has been carried out. However, more research on connection is very much requested in the papers that have been written on RFs so far, for example by Pugnale *et al.* (2011).

## 1.2 Aim and objective

### 1.2.1 Aim

The aim of this thesis is to investigate possible connection designs in RFs and thereby fill a gap in the current research. Their structural influence on the RF is of main interest but the thesis also examines the link between the connections and the production, assembly, disassembly and reuse and appearance. It will result in a classification of a number of connections types that have been used or could be used in RF structures. An evaluation of the types with regard to a number of indicators will be presented and two connection types will be presented more in detail in a structural context with their influence assessed in a finite element (FE) model.

### 1.2.2 Objective

To fulfil the aim of this thesis, the following questions will be answered. They are sorted in four groups which represent different phases of the thesis process: Background, Evaluation, Design/Analysis and Physical model.

#### 1.2.2.1 Background

- How has reciprocity been used for load bearing structures throughout history?
- What are the main parameters defining a RF?
- What element types and composition types can be identified?
- What connection types can be used in timber RF structures?

#### 1.2.2.2 Evaluation

- How can the connection be produced?
- Does the connection allow for easy assembly, disassembly and reuse?
- How is the appearance of the connection? Bulky or light?
- What are the structural properties of the connection?

#### 1.2.2.3 Design/Analysis

- What translational and rotational stiffness does the connection provide?
- How can the RF structure and the connection be modelled in a FEM software?

- How does the design of one connection type influence the structural behaviour of the overall structure, compared to another connection type?
- What member sizes and connection detailing would be needed in a particular structural context with a certain span?

#### **1.2.2.4 Physical model**

- How easy is assembly and disassembly?
- Does the structural behaviour of the physical model match the FE model?

### **1.3 Limitations**

In general, this thesis will only treat RFs with timber elements, since it is a material widely used in this type of structure. However, components in the connections and some general discussions might involve other materials to act as examples. The thesis will not go into detail regarding form finding and morphology of the overall RF composition since this has already been treated in several papers and to set a clear focus on the connections. In order to get a structure which is relatively easy to understand and results that can be communicated in a clear way, the chosen connection will be put in a flat composition. The dynamic response of RFs will not be covered, although this might be a suitable study to perform in the future.

### **1.4 Method**

As indicated above, the thesis process is divided in four main phases: *1. Background*, *2. Evaluation*, *3. Design/Analysis* and *4. Physical model*. During *1. Background*, relevant reference literature is read to get enough information to categorize element types, composition types and connection types. The connection types are then in *2. Evaluation* evaluated with regard to a number of indicators, such as production, assembly, disassembly, reuse and structural properties. From the evaluation, two connections are chosen for further analysis in *3. Design/Analysis*. The connection types are put in a context with a certain span and loads, and then designed and analysed. Their translational and rotational stiffness are assessed and used as input in a global model built in the FEM software Karamba where their influence on the structural behaviour of the RF is analysed. To verify the FE model and to evaluate production and assembly properties, a full scale model is realized in *4. Physical model*. A summary of the method is stated in the list below.

- Background: Collection of information, classification of types.
- Evaluation: Evaluation of the connection types. Two types chosen for further investigation.
- Design/Analysis: Design and analysis of the chosen connection types.
- Physical model: Building a physical model and perform tests.

## 2 Historical background

The principle of reciprocity has been used since ancient times. This chapter will go through the long history of RFs, starting from early related examples, continuing to medieval applications in Asia and Europe before describing an increased interest in the beginning of the twentieth century. Also some contemporary examples will be given.

### 2.1 Early use of reciprocity

Two early examples of structures showing similarity to RFs are the Indian tepee and the Hoogan dwellings (Popovic Larsen, 2008). Like RFs, they are both based on interlocking, mutually supported elements. The elements of the Indian tepee converges to one point where they are tied with a lash to ensure the stability of the structure. As weather protection and to add even more stiffness to the structure, animal skin is tensioned over the elements. The Hoogan dwellings also use a combined climate protection and stability component, namely mud between the beams. It glues the beams together and helps to keep them in place.

Another early example of a structure based on reciprocity is a bridge over the Rhine built during the Roman Empire by Julius Caesar (Pugnale & Sassone, 2014). The main purpose for using a reciprocal concept with interlocking beams for this bridge was to get simple connections that were fast to construct.

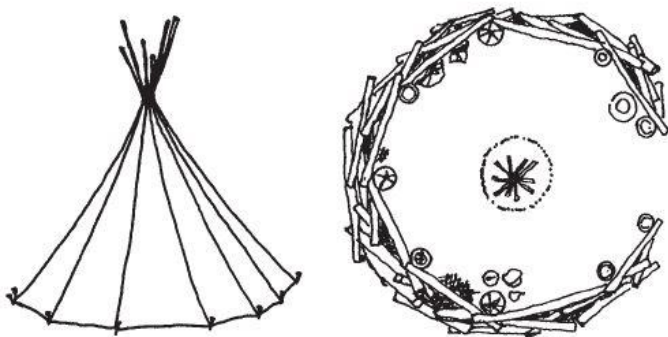


Figure 2.1 Indian tepee (left) and a Hoogan dwelling (right). [1]

### 2.2 Applications in Asia

The historical applications in Asia have two directions: one having a religious symbolism and one structural concept inspired by the traditional use of bamboo baskets (Pugnale & Sassone 2014). The former is mostly linked to Buddhist temples where circular shaped roofs has been desirable to highlight the meditation concept of mandala. Popovic Larsen (2008) states that there is a link between the spiral shaped RF roofs and mandala, where the meditating Buddhist strives towards the centre the ultimate holy state. There are unfortunately only documents as old as from year 1275 that proofs this religious application (Pugnale & Sassone, 2014).

The “Rainbow Bridge” in Shandong is an example of a structure inspired by the bamboo baskets with interwoven strips (Pugnale & Sassone 2014). This RF structure is at least 900 years old (Baverel, 2000) but has not remained until today.

## 2.3 Medieval and later structures in Europe

In Europe, early applications of RFs was for timber floors during the Middle Ages. Several architects and engineers during this period tried to figure out a good way to use beams shorter than the distance they would span. The French architect Villard de Honnecourt made sketches in the period between year 1225 and 1250 and they illustrate how four beams are placed to form an interlocking structure over a square perimeter (Popovic, Larsen, 2008).

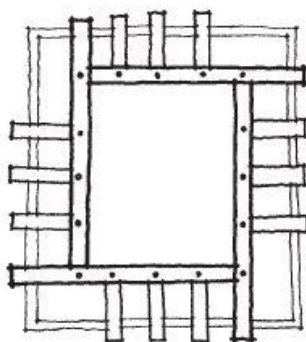


Figure 2.2 Honnecourt's four beam planar grillage. [2]

With identical sketches of a four beam composition, the next known designer to investigate RFs was Leonardo da Vinci who lived between year 1452 and 1519 (Popovic Larsen, 2008). But Leonardo also made sketches of more complex RF compositions such as a curved bridge design with interlocking beams. He also extended the concept with four beams to involve more beams in a floor grillage. After Leonardo, the Italian architect Sebastiano Serlio added contribution to the investigations of RFs when he proposed an extension of Honnecourt's composition (Pugnale & Sassone, 2014).

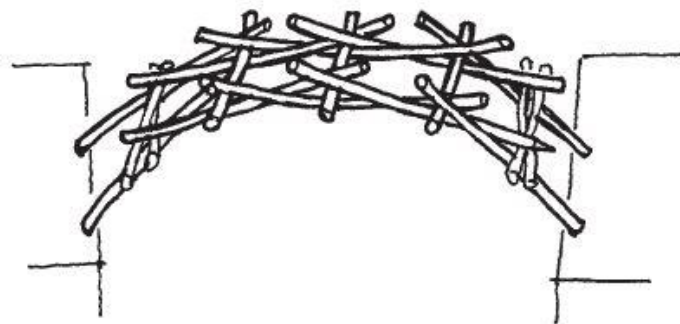


Figure 2.3 Leonardo's bridge design. [3]

Later European examples includes John Wallis' grillage structures that he presented in his work *Opera Mathematica* from 1695 (Pugnale & Sassone, 2014). An important part is the structural calculations that Wallis made for the structures and this is the first scientific contribution in the RF history. Popovic Larsen (2008) calls this “the first known written document exploring the load transfer of the structure”. In 1841, professor Émy of Fortification of the Royal Military School in Saint-Cyr, presented additional flat planar grillage and in 1890 Thomas Tredgold made comments on previous presented RF structures (Pugnale & Sassone, 2014).

## 2.4 Scientific research in the twentieth century

Pugnale & Sassone (2014) points out that an increased interest and scientific research of RFs in the twentieth century started by a RF system made by the designer Graham Brown, first patented 1989. But a number of patents related to RFs were already registered at that time, for example the joint by the German engineer Friedrich Zollinger from 1924. Zollinger's intention was to create a connection in a lamella dome that could be constructed quickly, and this was achieved by avoiding that the elements meet in a single point. Instead they form a RF joint with offset beams and only two elements meeting in a node (Popovic Larsen, 2014). After the First World War there was a serious lack of housing and the speed of construction in Zollinger's system played an important role in solving that problem.

In the 1960's, Emilio Perez Piñero registered a patent for a foldable RF structure and in the 1970's two German engineers registered a system with prefabricated concrete units. The 1970's was also the time for the first RF system to be published in a scientific journal (Pugnale & Sassone, 2014). It was the SIGMA system, patented by Daniel Gat in 1981, which was a pure refashioning of Wallis grillage from the eighteenth century (Baverel, 2000). One difference though, was that Gat added a wedge component, allowing the structure to form a 3D composition.

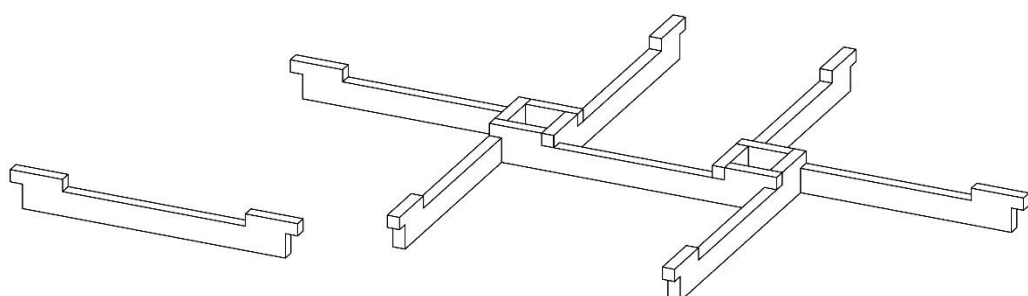


*Figure 2.4 Element and simple composition illustrating the concept of Daniel Gat's SIGMA system.*

The above mentioned Graham Brown was actually the person to give the structure Reciprocal Frame its name (Popovic Larsen, 2008). He collaborated with researchers from the University of Nottingham to increase his understanding of RFs and that resulted in several publications made together with Dr John Chilton, for example a

Ph.D. thesis on the subject made by Olga Popovic Larsen in 1996 (Pugnale & Sassone, 2014).

## 2.5 Contemporary examples

In Japan, RF structures have been used for a number of different buildings. One famous example is the Bunraku Puppet Theatre, built between 1992 and 2002 and designed by the architect Kazuhiro Ishii (Thönnissen, 2015). It consists of a number of different buildings, including the auditorium shown in the figure below. The beam grillage is quite heavy, measuring over one meter in height at the points where the beams intersect. The reason why this heavy RF timber structure was chosen for the auditorium was to express the sad stories in the plays performed on the stage, according to Ishii (Popovic Larsen, 2008). Every element of this structure rests on another element in one end and are suspended in the other end using a steel anchor (Thönnissen, 2015).



Figure 2.5 The auditorium at Bunraku Puppet Theatre by Kazuhiro Ishii. [4]

Alvaro Siza's Serpentine Gallery Pavilion from 2005 has connections with similarities to the Zollinger joint (Jeska & Pascha, 2014). With the Zollinger joint concept, only two elements meet in one node, allowing for very simple connections. To make it possible to use a so called mortise and tenon joint, which is described further in chapter 4, high strength laminated veneer lumber was used.



Figure 2.6 Zollinger-like connections in Alvaro Siza's Serpentine Gallery [5] Pavilion.

In Bibracte, France, a RF structure made of aluminium was used to form a cover of an archaeological excavation site in 2008. The reason why a RF structure was chosen was because of RFs low sensibility to settlements, since the ground of the site was assumed to be soft and irregular (Gelez, Aubry & Vaudeville, 2011). Additionally there was a demand on simple assembly and disassembly, and hence, the short elements of the RF was suitable. Pinned connections could easily be created and absence of geometrical blockage limited the need for advanced tools on site.

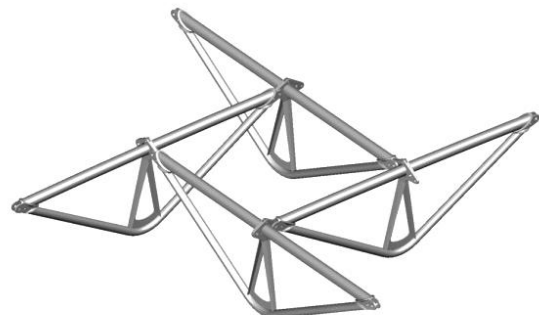


Figure 2.7 Photo of archaeological excavation site in Bibracte (left). [6] Drawing of a reciprocal frame unit of the roof structure (right).

Professor Annette Spiro of ETH in Zürich, Switzerland has carried out extensive research on RFs together with the architect Udo Thönnissen. Spiro points out the potential of RF structures as a new construction technique to use hardwood, which is a promising timber type thanks to its low cost (Spiro, 2012). Several pavilions have been designed and built by Spiro's team, for example the Piazza HIL. The pavilion consists of 120x120 mm timber beams which are connected with notched joints.



*Figure 2.8 Piazza HIL pavilion, designed by Annette Spiro's team at ETH [7] Zürich.*

### 3 Elements and compositions

The elements used in timber RF structures can have several different geometries that each give certain possibilities and restraints to the compositions. This chapter will present the elements together with their different properties. In order to understand these properties, the fundamental parameters of a RF will be introduced in the first section. The two main composition types, flat and curved, will also be described.

#### 3.1 Fundamental parameters

When the elements are put together they can form a closed RF unit called a fan. This RF fan is defined by six parameters (Thönnissen, 2014): The *style of the fan*, the *number of elements* in the assembly, the *eccentricity* between the elements centroid axes, the distance between the point where an element is supported and the point where it supports another element – called the *engagement length*, the *element length* and the *composition* of members in the structure. Since every element is dependent on every other element and their corresponding parameters, changing a single value will affect the entire structure (Thönnissen, 2014).

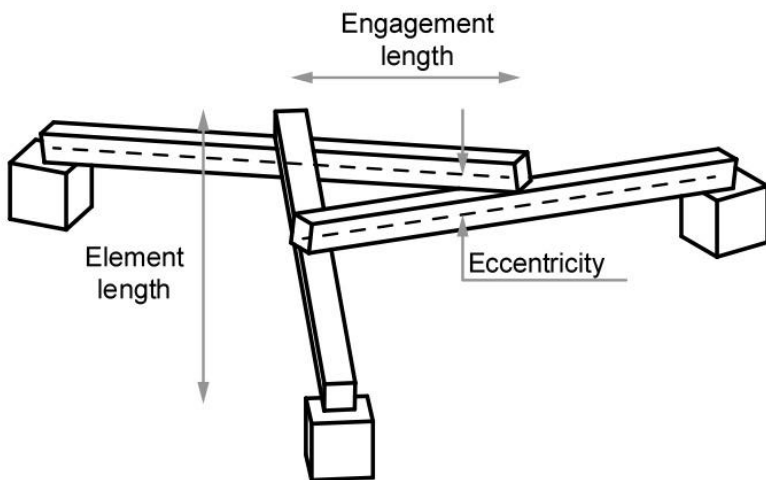


Figure 3.1 Parameters defining a RF composed by elongated elements. The eccentricity is measured between the centroid axes of the elements (dashed lines).

#### 3.2 Elongated elements

Elongated elements are elements that extend along one major axis. Depending on the proportions between width, height and length, as well as the angle between the faces of the elements, elongated elements can be subdivided into rods, panels and blocks.

##### 3.2.1 Rods

Rods are slender, slat-like elements. Due to their low height, the eccentricity between two elements in a fan can be kept low, even without a notch in the elements.

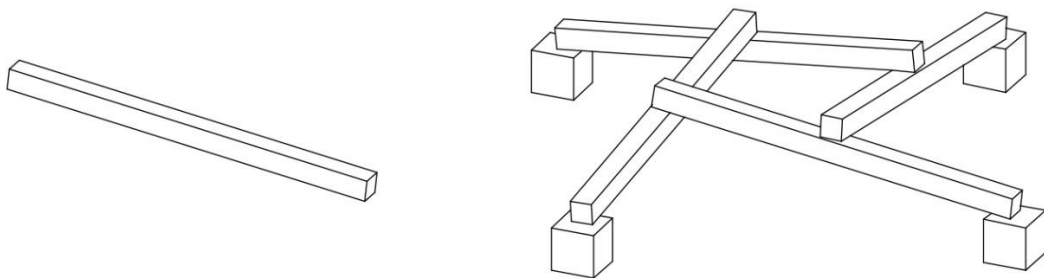


*Figure 3.2 Rod element and a four element fan on four supports.*

### 3.2.2 Panels

Thin but high elongated elements can be defined as panels. Due to their height, panels generate a very high eccentricity between the elements if put directly on top of each other and hence they are most often notched. The height also creates a less transparent fan than a fan composed by slender rods which make the panels suitable to use as a shading structure for the space below the fan.

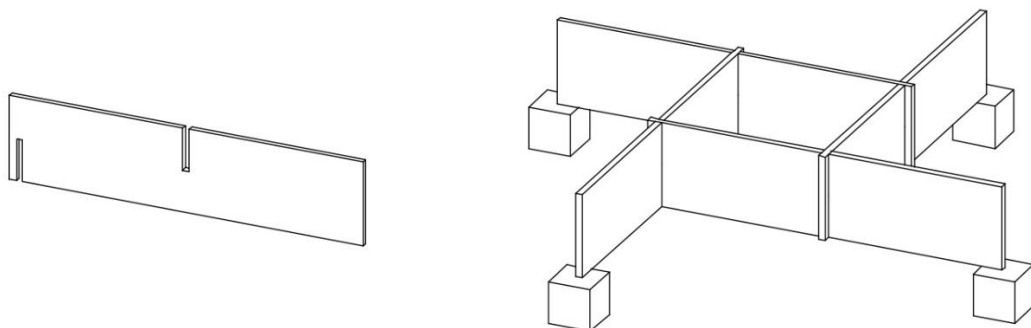


*Figure 3.3 Panel element and a four element fan on four supports.*

### 3.2.3 Blocks

Block elements have a relatively short length compared to their width and height. They are often used together with angled faces to create interlocking fans. J. Abeille made investigations on RF configurations with block elements in the eighteenth century (Baverel & Popovic Larsen, 2011). Abeille's work shows how block elements can form a nearly solid floor slab which closes the engagement window.

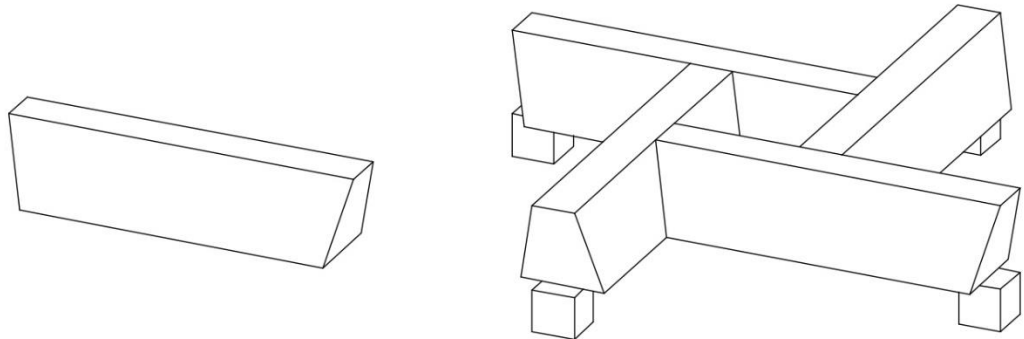


*Figure 3.4 Block element and a four element fan on four supports.*

### 3.3 Plate elements

Plate elements spread out in two major directions, which means that they are relatively wide and long but only have a small height. The plates can be notched in order to form an interlocking fan or be bent if they are flexible enough. Similar to the block elements, plates can generate a fan which fully covers a span and the elements can serve both as structure and cladding.

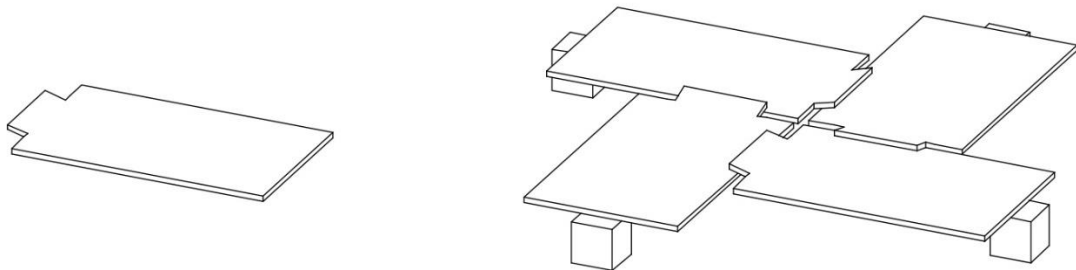


*Figure 3.5 Plate elements and a four element fan on four supports.*

### 3.4 Ring elements

The same parameters that governs a RF consisting of elongated elements defines a composition with ring elements (Baverel & Popovic Larsen, 2011), but these elements all form a closed circuit. The ring elements can be connected in a number of different ways to form an interwoven configuration.

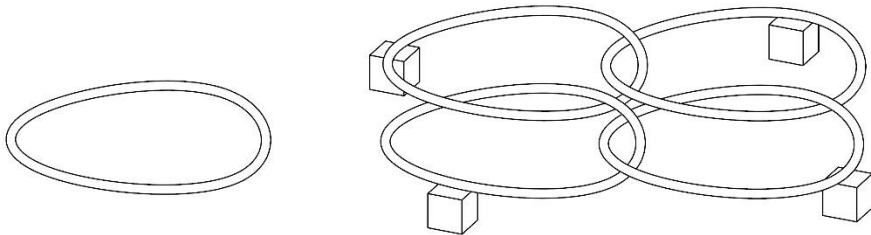


*Figure 3.6 Ring element and a four element fan on four supports.*

### 3.5 Combinations and alterations

The elements presented above can also be combined with each other, creating elements that have properties of several elements. For example a panel element can be combined with two plates in the transversal direction to form a larger element with extended interlocking properties, as in Figure 3.7. The combined element has the high in plane bending stiffness of the panel and the ability to cover an entire span with cladding thanks to the plates. The elements can also be 3D trusses which brings a possibility to easily connect the elements to each other in the gaps of the trusses.

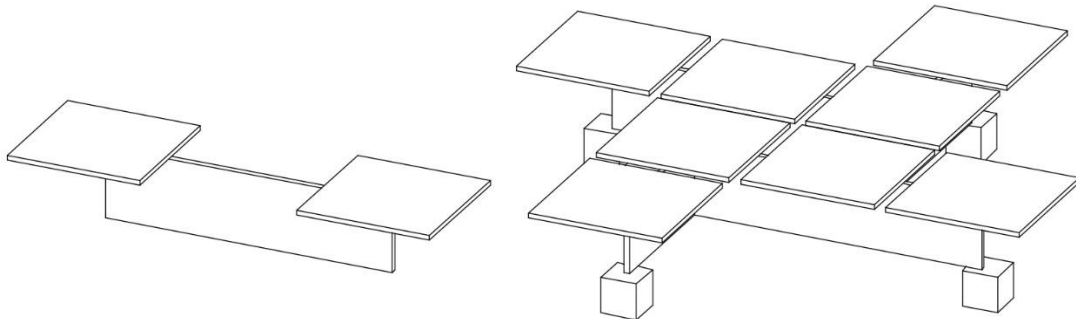


*Figure 3.7 Combined panel and plate element and a four element fan on four supports.*

### 3.6 Compositions

From the minimal basic composition of the elements, the fan, larger RF structures are formed by connecting several fans. Depending on the eccentricity of the elements they form either a flat or a curved composition.

#### 3.6.1 Flat compositions

For flat compositions the eccentricity between the centroid axes of the elements equals zero (Thönnissen, 2014). The structure spreads out in a two-dimensional, planar formation and floor slabs, flat roofs and walls are possible building parts for

which the composition type is suitable. The earlier mentioned examples sketched by Honnecourt, da Vinci and Serlio are all flat compositions.

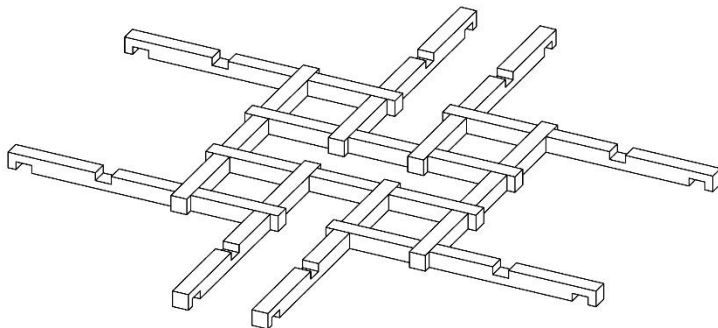


Figure 3.8 Flat composition. Zero eccentricity achieved with notches.

### 3.6.2 Curved compositions

Curved compositions have, in comparison to flat composition, an eccentricity larger than zero which is achieved by inclined elements superimposed on top of each other. In this way a three dimensional structure is created and it can serve as a space in itself without any need for additional walls etc. Hence, curved compositions can be suitable in situations where there is no demand on keeping the structure flat, for example pavilions, hall buildings etc. An obvious advantage with curved compositions is that they can be optimized to transfer the load in compression and tension to a larger extent than in bending. However, the elements will still be subjected to some bending moments and shear forces (Popovic Larsen, 2008), due to inherent properties of RFs.

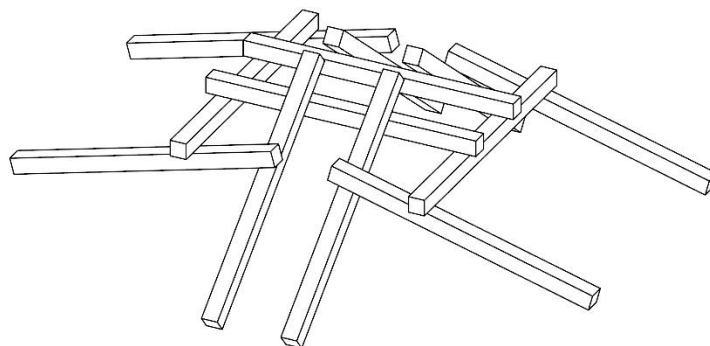


Figure 3.9 Curved composition. Eccentricity achieved by superposition of elements.

## 4 Connection types

This chapter introduces the main focus for this thesis, the connections used in RF structures. Four main types can be identified: Superposition, Couplers, Dowels and plates and Notches. Sub-categories within each type and the production method, assembly, disassembly, reuse, appearance and structural properties will be listed.

### 4.1 Superposition

The elements are simply placed on top of each other in a superposition connection, and it relies entirely on the interlocking effect of the elements in a RF composition. Vertical loads can be transferred as shear in one direction and in the opposite direction the element have to be secured against lifting (Thönnissen, 2015). For horizontal loads, the friction at the contact surface of the elements is what keeps the elements in place.

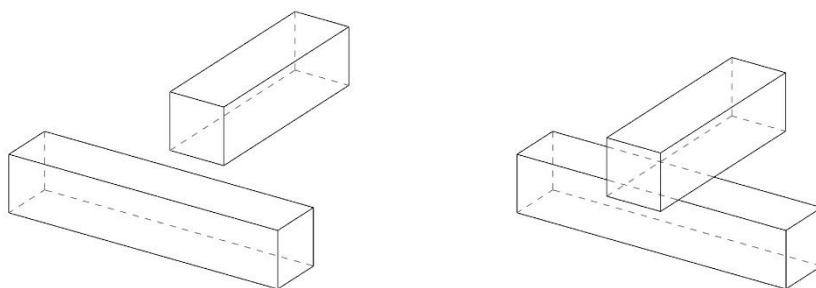


Figure 4.1 Superposition connection by pure superposition.

#### 4.1.1 Pure superposition

The elements can simply be placed on top of each other. For RFs with this kind of connection, production and assembly is relatively easy since there is no need to apply an additional connector component. But since the elements stay in position only due to the friction, the assembly can be troubled by the fact that the structure does not function before all the elements are in place. Also, if the elements are inclined, small gaps will form between the elements which decreases the contact area.

#### 4.1.2 Superposition with wedges

To avoid the gaps between the elements a small wedge can be built on the beams. If the wedge is integrated with the element, this of course complicates the production of the element somewhat but makes the assembly easier. Also, the cross section increases when the wedge is added which increases the structural capacity.

#### 4.1.3 Production

Since the pure friction type of connection does not require any additional connection component or only little treatment of the element itself (for the wedge-type), basically no production or preparation for the connection need to take place. The connection is

established when the elements are simply put on top of each other and the structure is interlocked.

#### 4.1.4 Assembly, disassembly and reuse

As Pugnale & Sassone (2014) states, the assembly can be considered as very easy since no additional component is needed but on the other hand it can be complicated by the lack of stiffness in the connections. Temporary supporting structures are very often needed due to the fact that the composition is not stable until the last element is in place. This is not only an important aspect to keep in mind during assembly but also during disassembly since removing one element will allow the other elements to move out of place.

Of course the degree of complication depends on the scale of the structure and the availability of machines, temporary structure, workers etc. Even a small model composed by only four elements can be quite difficult to assemble for one person alone. A possible assembly method is to start with a simple fan of three elements and then add more elements to build more complex compositions.

A strength with this connection type is that it allows the elements to form other composition types when reused after disassembly. The elements are not damaged by nails or any other connector component.

#### 4.1.5 Appearance

The absence of an additional connection component gives a very clean appearance, the element does not need to blend with a connector and the timber can be kept homogenous. However, since this connection type demands that the elements are placed on top of each other, the elements need to be inclined if they are shaped as straight, for example rod elements extending along one axis, as in Figure 3.9. This breaks the horizontality of the structure and gives it a certain character. An S-shape, as in Figure 4.2, is a possible way of keeping an orthogonal character of the composition. With the S-shape, the top surfaces of the elements are on the same level and hence the composition might be easier to clad than a composition with inclined elements.

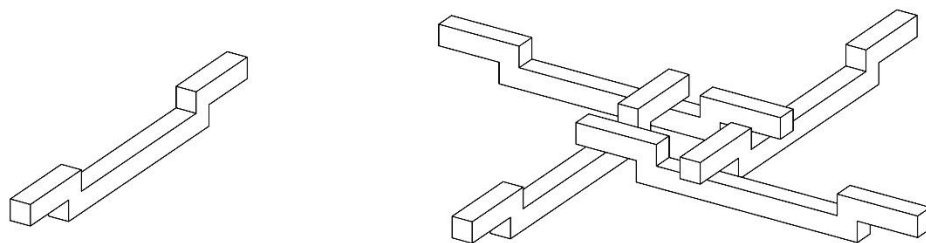


Figure 4.2 Element and fan with superposition connection.

#### 4.1.6 Structural properties

As stated earlier, vertical loads are transferred by shear, whereas the horizontal stability relies on the friction between the elements. Since the connection is based on the interlocking effect that the elements create together, removal of one element can cause a collapse of the entire structure (Popovic Larsen, 2008) and this makes it very fragile.

#### 4.1.7 Built example

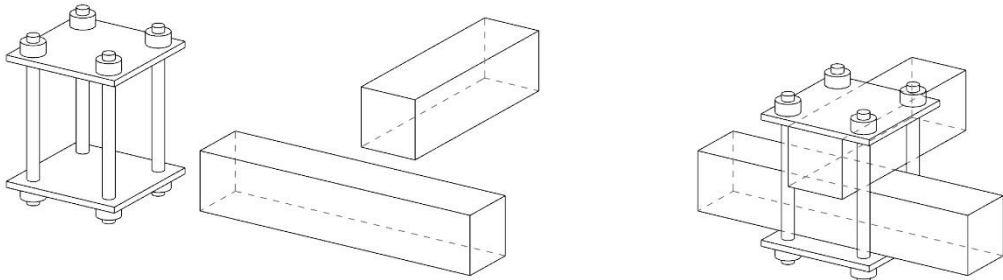
During the research of this thesis, no large scale timber RFs with superposition connection has been found. Nevertheless, Attilio Pizzigoni, associate professor at University of Bergamo has carried out research on a RF structure with fibre-reinforced concrete elements. This structure has S-shaped elements which simply rests upon each other, resulting in a superposition connection based entirely on friction and the interlocking effect of the RF. The research, which includes both an extensive FEM analysis as well as tests of physical, full scale fans, concludes that the RF with this connection is as structurally effective as a “traditional” structure (Garavaglia et al., 2013). A “traditional” structure seems to mean a structure with zero engagement length where not only two elements meet in one node. Only scaled models of an entire composition has been realized but Pizzigoni presents a design proposal for the Italian World Expo Pavilion in Shanghai 2010 (Pizzigoni, 2009). The structure has a waterproof, transparent cladding attached from underneath and provides both shading and weather protection.



Figure 4.3 Pizzigoni's proposed structure (left) and a scaled model (right) [8] with superposition connections.

## 4.2 Couplers

By using an additional component, this family constrains the elements to a various degree. It can look in a number of different ways, each with different properties.



*Figure 4.4 Coupler connection with a clamp-like connector.*

#### 4.2.1 Lashing

This type of connection was often used in early examples of RF structures. The lashing wire can be made out of several different materials, such as steel and various fibres which of course will have an impact on the ultimate strength on the structure. The assembly can be eased by drilled holes in the elements where the wire can be lead through. In this way a geometric flexibility is created, leaving a margin for putting the elements together. Such a connection constrains translation of the elements but allows rotation (Gelez & Saby, 2011).

#### 4.2.2 Contractible clamps

This is a common type of connection in construction scaffolds with steel tube elements, but it is also possible to use with timber elements. Like the lashing, the clamps builds a connection by increasing the friction grip to transfer load (Rizzuto & Popovic Larsen, 2010). Major advantages are that the clamps can create a connection in any kind of angle and that they ease assembly and disassembly (Rizzuto & Popovic Larsen, 2010).

#### 4.2.3 Joist hangers

A common timber to timber connection is to fasten a joist hanger, often a metal component, in one of the elements and then let the other element rest on the hanger. The joist hanger then constrains the supported element for rotations and translations. Recent examples from furniture design show 3D-printed plastic connectors similar to joist hangers.

#### 4.2.4 Production

Except for the joist hangers, the production of the connection components in this family does not need detailed information about the elements since the lashing wires and the clamps can be adjusted to the sizes, angles etc. The joist hangers, especially the plastic connectors which are made fix in a certain angle, need to be produced customized to the element properties. On site, the connections are formed by applying the couplers at the intersection of two elements.

#### 4.2.5 Assembly, disassembly and reuse

To assemble a structure by lashing the elements together is very simple with predrilled holes in the elements, since this leaves a margin in creating the geometry, which can be very complex for curved compositions (Gelez & Saby, 2011). On the other hand, without predrilled holes, the lashing has to be a little more advanced to create a connection with sufficient stiffness. Disassembly of a structure connected by lashing, is simply made by cutting the wires and this causes no damage on the elements which allows for reuse, which has been made in several student workshops on The Royal Danish Academy of Fine Arts Schools of Architecture (Popovic Larsen, 2014). Assembly and disassembly is also relatively easy performed with clamps, which as lashing wires leaves no damage on the elements.

The traditional joist hangers need to be connected to at least one of the timber members with some kind of dowel connector that will damage the element. However, if vertical translations and rotations could be accepted, the element supported by the hanger does not need to be connected with dowels. This could ease both assembly and disassembly with a higher degree of reusability of the elements.

#### 4.2.6 Appearance

Since the coupler type connection introduces a second component it gives a less clean appearance than the connection types based on friction or notches. There is a risk that the component is perceived as bulky and takes its toll on the simple beauty of the interlocking RF. However, this component, with its own materiality and character, could be highlighted to contribute to an appealing composition. It could also be integrated with cladding to make it less visible and bulky. Another strategy is to make it very subtle and make it blend into the elements. The couplers, given straight elements, generate a curved structure. But as for the superposition connection, the element can also be varied, as in Figure 4.5, to create a flat structure.

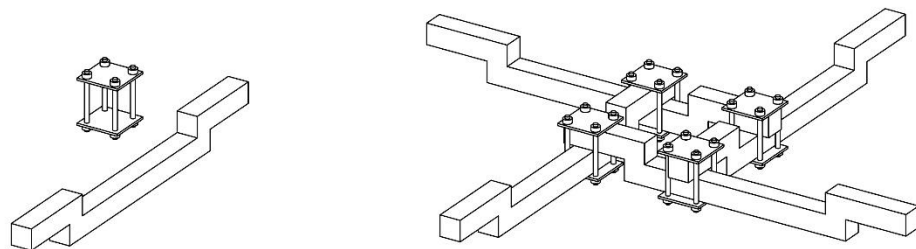


Figure 4.5 Element and a fan with a contractible coupler connection.

#### 4.2.7 Structural properties

This family of connections all create an eccentricity between the element's centroid axes. This eccentricity has a major impact on how the forces, moments and stresses are distributed between the RF elements (Rizzuto & Popovic Larsen, 2010).

The lashing is described by Gelez & Saby (2010) as a relatively flexible connection, allowing rotation but blocking translation. It is of course possible to add more

constraints by adding additional ties, as Popovic Larsen (2014) suggests as measure to stiffen a RF structure produced in a workshop with 1 m long timber rafters with predrilled holes.

#### 4.2.8 Built example

The builder Tony Wrench has established a concept which he calls Roundhouses (That Roundhouse, n.d.). The Roundhouses are used as residential homes or simple dens and have a RF roof where timber rafters are placed in a spiral pattern, successively supporting and interlocking each other. The diameter of a den can be 5-6 meters without internal supports. Tony Wrench originally used telephone wires to create a lashed connections of the rafters in the RF but for a Roundhouse in France he used jute rope (Mr T. Wrench, 2016, pers. comm., 15 March). For all major joints in this Roundhouse, an oak peg of 18 mm was used in addition to the rope. The top circle where the rafters meet was encircled seven times with the rope.



Figure 4.6 Roundhouse in France by Tony Wrench during construction. [9]



Figure 4.7 Lashed joint of a Roundhouse in France, using jute rope. [10]

### 4.3 Dowels and plates

Dowel type and plate fasteners refers to connecting the elements with an additional component which is punched into the elements, penetrating them both, thus allowing forces to be transferred between them.

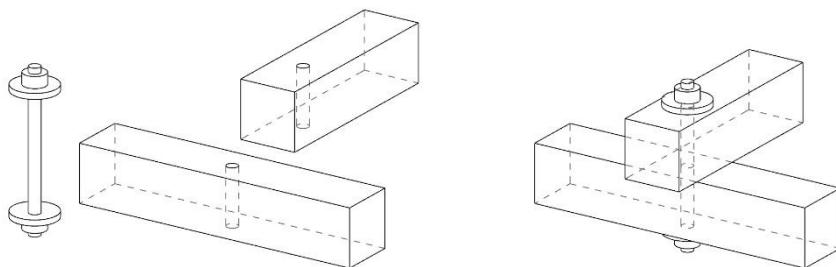


Figure 4.8 Doweled connection with a bolt.

#### 4.3.1 Pure dowels

Dowels are cylinders without a head and a diameter larger than 8 mm (Swedish Wood, 2011). Dowels are punched into predrilled holes in the timber elements to connect. Using dowels by a stronger wood type than the type used for the rest of the beam is an old way of establish a connection in timber structures.

### **4.3.2 Nails and screws**

Nails are smooth or rugged cylinders with head diameter smaller than 8 mm which is punched directly into the wood or into a predrilled hole (Swedish Wood, 2011). Screws are also cylinder with a head but separates from the nails by having a threaded surface.

### **4.3.3 Bolts**

Bolts are like a mix of a screw and a dowel, being a cylinder with a threaded surface, often the lower part, a head and a diameter larger than 8 mm. Generally a nut and a washer is added to the bolts to achieve sufficient anchorage (Swedish Wood, 2011).

### **4.3.4 Plates**

There are several plate type connection components. One common type is the punched metal plate which is often categorized as a dowel type fastener since it has a number of nails which are formed by folds in the plate. Since the punched metal plate is pre-fabricated with the folded “nails” sticking out of the plate, it can be used directly and automatically fulfils the code requirements with regard to spacing. This type of plate is however most often attached with a hydraulic press and not very practical to use for construction on the building site, i.e. not very suitable for RFs that are not prefabricated. The nails of the punched metal plate has low capacity since they are only 2 mm thick due to folding demands (Swedish Wood, 2011).

Tooth-plates are available in a number of different shapes and can be either single- or double sided. The strength of this connection type is depending on both the capacity of the tooth-plate connector and the capacity of the bolt that ensures the embedment in the timber (Porteous & Kermani, 2013). For structures with a demand on being demountable, a double sided tooth-plate is preferable.

According to Porteous & Kermani (2013), split-rings and shear plates are connectors with a significantly higher bearing capacity than the tooth-plates. They are mounted into pre-fabricated grooves in the timber and unlike the tooth-plates, the bolt does not contribute to the joint strength.

A possible way of creating a connection very much integrated with the timber element is to use a slotted-in steel plate. This hides the connection within the element and is also good from a fire protection perspective, since steel components are very sensitive to high temperatures. Slots for the steel plates are cut in the edge of the element and holes are drilled through the steel plate and the element where dowels are inserted (Swedish Wood, 2011).

### **4.3.5 Glued-in rods**

Another way of hiding the joint within the element is to place a steel rod at the end of the element and fix it with glue. The rod can then be inserted into another element to form a very strong and stiff connection (Swedish Wood, 2011).

### 4.3.6 Production

The connection types in this family all demand some preparation before the assembly, regardless if it is the production of dowels or more advanced plate type connections with pre-fabricated grooves in the elements. On site, the connection is formed in very different ways depending on which dowel or plate type that is used, but the overall procedure is to create the link element-fastener-element.

### 4.3.7 Assembly, disassembly and reuse

To assemble a RF structure with dowels can be very quick and easy, especially if the geometry of the composition generates no, or only a small distance between the elements. Since for example nails or screws directly establish a connection that can transfer load, the structure can function to some degree before it is completed. The structure can be built in parts and then assembled to form a complete, linked structure.

The disassembly is however complicated by the fact that many of these components are relatively difficult and time consuming to remove from the timber, once in place. However, some of the connection types, for example bolted connections, could be released relatively easy without damage to the elements except from the predrilled hole.

### 4.3.8 Appearance

From an appearance perspective, this connection family is very diverse: from bulky bolted connections to delicate nailed joints that are hardly visible. Also, there are examples of connections that can be integrated within the elements to form a fully hidden joint.

Of course this connection type, as the couplers, need to be combined with notched or S-shaped elements to form a flat configuration of the RF structure. Otherwise the elements need to be inclined.

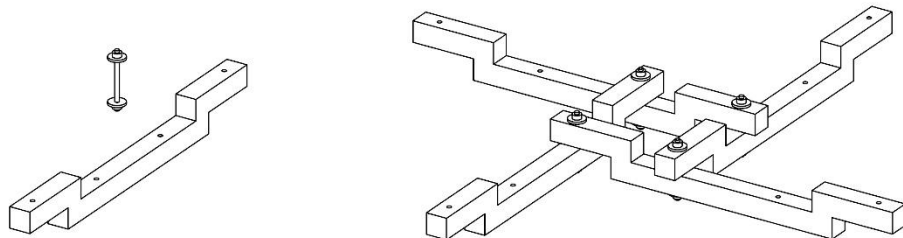


Figure 4.9 Element and a fan with a bolted doweled connection with predrilled holes.

### 4.3.9 Structural properties

The dowels act as a beam when they transfer the load, which is most often acting perpendicular to the direction of the dowel (Swedish Wood, 2011). Three parameters decide the strength of a dowel type connection: the embedding strength of the timber, the dowel strength and the anchorage capacity. The two latest depend on the material of the dowel, today most often steel, and how it is designed.

Translation is generally constrained by dowels and plate connectors, but the rotational stiffness can vary. For example an element can rotate around one nail, but adding another nail will prevent the rotation to a larger degree. Also, the degree of fixation due to the dowel can change over time. In research for a RF roof truss, the doweled connections were modelled as pinned because they were assumed to become loose over the years (Popovic Larsen, Lee & Lange, 2014).

A positive property of this type of connection in complex, indeterminate timber structures is that they can allow a ductile behaviour (Aicher, Garrecht & Reinhard, 2014).

### 4.3.10 Built example

For the Kreod Pavilion that was designed for the London Olympic Games, a reciprocal configuration for the joints was chosen as a way to reach simple connections. Naturally, only two elements meet in one node and the structure is easier to assemble and disassemble than other similar structures (Popovic Larsen, 2014). The elements are connected using a bolted joint with a cam lock, similar to connections in furniture design.



Figure 4.10 Kreod Pavilion. [11]



Figure 4.11 Bolted connection in Kreod Pavilion. [12]

## 4.4 Notches

By making a notch in the elements one can make connections that are integrated in the element. The different sub-families differ in the production demand, the assembly technique and structural properties, such as what kinematical constraints they can provide to the structure. They all have one thing in common regarding the appearance: the connection is integrated in the elements without an additional component.

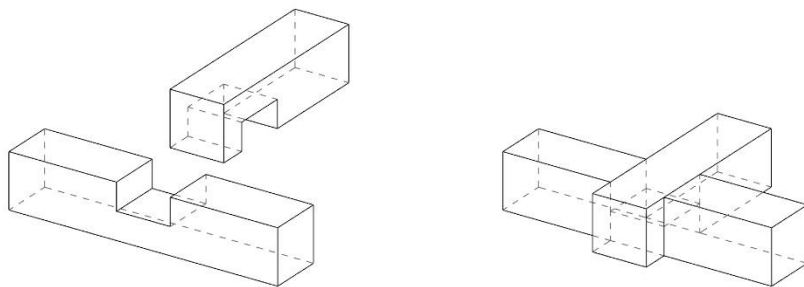


Figure 4.12 Notched connection with a half lap joint.

### 4.4.1 Half lap joints

Half lap joints can be designed in a number of different ways, but the common denominator is that the element to be supported sits on the lap of the supporting element. The design of the tail of the supported element, as well as the design of the lap of the supporting element, sets the properties of this kind of connection. Depending on the contact between the faces of the two elements, this connection can be more or less rigid.

#### **4.4.2 Mortise and Tenon joints**

Instead of sitting on the lap, Mortise and Tenon connections have the supported element going into the supporting element. In a so called Through Mortise and Tenon Joint the supported element goes all the way through the supporting element, and if it sticks out on the other side, it can even be locked with a wedge, forming a Tusk Mortise and Tenon connection. If the supported element does not go all the way through, the connection is called a Blind Mortise and Tenon joint. This kind of design hides the hierarchy and the interaction of the elements entirely.

#### **4.4.3 Production**

Notches can be pre-cut in a factory before the elements are transported to the buildings site (Rizzuto & Popovic Larsen, 2010). If there is a demand on very tight connections, the notches need to be very precise or the structure will not be able to put together (Popovic Larsen, 2008). Traditionally the production of notches has been made by hand and been very time consuming. Today, with digital tools such as CNC-machines, notches can be created much easier with a very high precision.

#### **4.4.4 Assembly, disassembly and reuse**

As stated for the production, it is very important that the notches are made in the correct way for the geometry to fit during assembly. If the notches are correctly cut, the assembly can be very quick and easy. Depending on the notch type, the assembly can be eased by moment resisting connections, adding stiffness to the structure before it is complete.

The disassembly is very much eased by the fact that there is no additional component, such as a clamp or screw, which needs to be removed. For very deep notches in for example planar elements, removing the first element might be complicated since this involves a relatively large translation that will generate increased stresses in the structure.

The reusability is generally very high for structures using notched connections. The elements are not damaged during assembly or disassembly and can be put up somewhere else. Over time, however, there is a risk that the connections start to lose their performance due to gap formations, for example related to shrinkage of the timber (Shiratori, Komatsu & Leijten, 2008). Another thing to keep in mind is that one notch design often generates a limited amount of compositions that the elements can form.

#### **4.4.5 Appearance**

A notched connection is integrated in the element, leaving a possibility to keep material homogeneity. Elements connected with notches generally seem to blend with each other and creates curiosity of what is happening at their intersection. Unlike the previously described connection types, notched connections make it possible to create a flat composition without using S-shaped elements. Hence, notched connections can create structures where every surface is on the same level, being very easy to cover with cladding, either on the top or from the bottom.

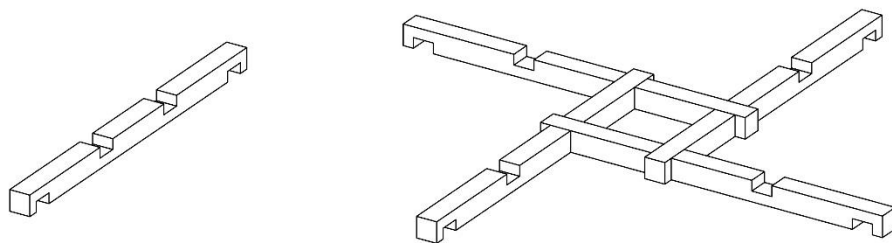


*Figure 4.13 Element and a fan with notched, half lap connections.*

#### 4.4.6 Structural properties

Since the notches will decrease the cross section of the members they will also decrease their load bearing capacity. Reducing the cross section along the length of an element will be critical with regard to its bending capacity while a notch in the end of the element will be critical with regard to its shear capacity (Rizzuto & Popovic Larsen, 2010).

Notched ends have a tendency to fail by brittle splitting in tension perpendicular to the grain (Aicher, Garrecht & Reinhard, 2014). The risk of such a failure can be limited by adding screws or cross veneers as reinforcement perpendicular to the grain.

Swedish Wood (2011) claims that the load transfer of traditional timber joints is limited and that the application is limited to short span buildings and furniture. However, one advantage with traditional notched connections is that they are based on compression perpendicular to the grain and that the structure has relatively large capacity of enduring lateral loads without sudden brittle failure (Shiratori, Komatsu & Leijten, 2008).

#### 4.4.7 Built example

The architect Kazuhiro Ishii has designed several buildings using RF structures with notched connections. One of them is the Seiwa exhibition hall which is a part of the Bunraku Puppet theatre complex in Kumamoto, southern Japan. The RF roof structure spans 8 m and utilizes a notched Japanese carpentry joint called “Vatariago” (Popovic Larsen, 2008).



Figure 4.14 Seiwa Exhibition hall by Kazuhiro Ishii. [13]

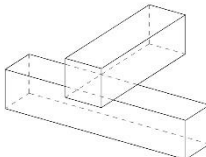
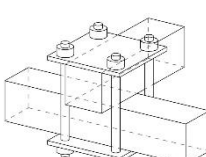
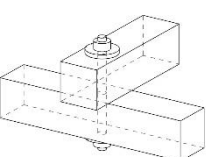
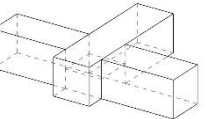


Figure 4.15 Notched Vatariago connections for Seiwa Exhibition hall. [14]

## 4.5 Summary of evaluation

The table below summarizes the pros (+) and cons (-) for each connection type. It can be concluded that all the connection types show approximately the same amount of pros and cons for the evaluated parameters. Although, it should be noted that this is just a brief summary and is not intended to point out what connection is the ultimate connection for use in RFs. Every structure has its own unique context where the different properties of the connections are desirable.

*Table 4.1 Summary of the evaluation of the connection types.*

				
	<b>Superposition</b>	<b>Couplers</b>	<b>Dowels</b>	<b>Notches</b>
<b>Production</b>	+ No production of additional component	- Production of additional component	- Production of additional component	+ No production of additional component - Notches complicated to produce
<b>Assembly, disassembly and reuse</b>	+ No damage to elements + Elements can form several compositions - No stiffness before complete assembly	+ No damage to elements + Elements can form several compositions + Quick assembly	+ Elements can form several compositions + Quick assembly - Some damage to elements	+ Quick assembly - Gap formations over time - Deep notches complicated to assemble
<b>Appearance</b>	+ No disturbance by additional component - Elements need to be inclined	- Disturbance by additional component - Elements need to be inclined	- Elements need to be inclined	+ No disturbance by additional component + Elements can be flat
<b>Structural properties</b>	+ No reduction of cross section - Not stiff - Low robustness	+ Stiff + No reduction of cross section	+ Stiff - Small reduction of cross section at dowel	+ Stiff - Large reduction of cross section at notch

## 5 Connection analysis

To understand how the connections influence the structural behaviour of the overall composition, their translational and rotational stiffness is assessed. These stiffnesses are then used as input to a global RF model. Two different connections have been chosen for this further analysis, one superposition and one notched connection. Since the members of the superposition connection can move almost entirely free in relation to each other, whereas the members of a notched connection can be very much locked to each other, they have the potential of influencing the RF in a diverse way.

### 5.1 Context

To see how the connections influence the structural behaviour of a RF they are put in a roof structure, spanning 5x5 meters. This roof could possibly be used to cover an exhibition stand, a structure that could benefit from using a RF for a number of different reasons:

- Short members are easy to transport and to handle on site. A site for an exhibition stand can be quite limited and hence short members can be handy.
- Since RFs make it possible to use simple connections where only two elements meet they can easily be designed for disassembly. Exhibitions stands are temporary structures and for sustainable reasons it is favourable if they can be reused.
- The simple connections also speed up the construction.

The connections are put in a common RF-pattern, seen in Figure 5.1, and the elements form a flat structure.

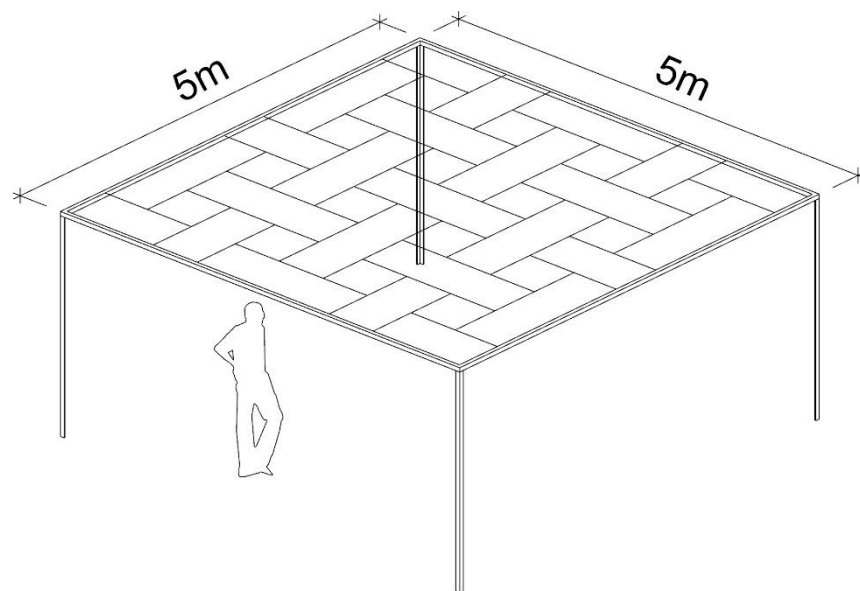


Figure 5.1 Structural context and pattern of the RF for the connections: A roof structure, possibly for an exhibition stand, with 5x5 m span.

## 5.2 Superposition connection

As mentioned in the connection evaluation, the superposition connections demand some kind of modification of the element in order to create a flat composition. In this case, an S-shaped element has been chosen which makes it possible to keep a horizontal expression of the composition. The element shape displays the way the beams interact and highlights the weaving character of the structure.

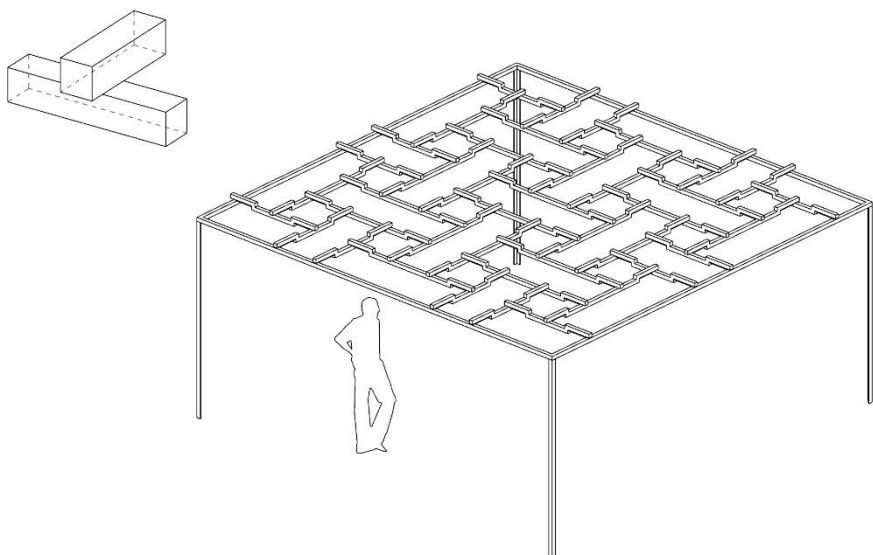
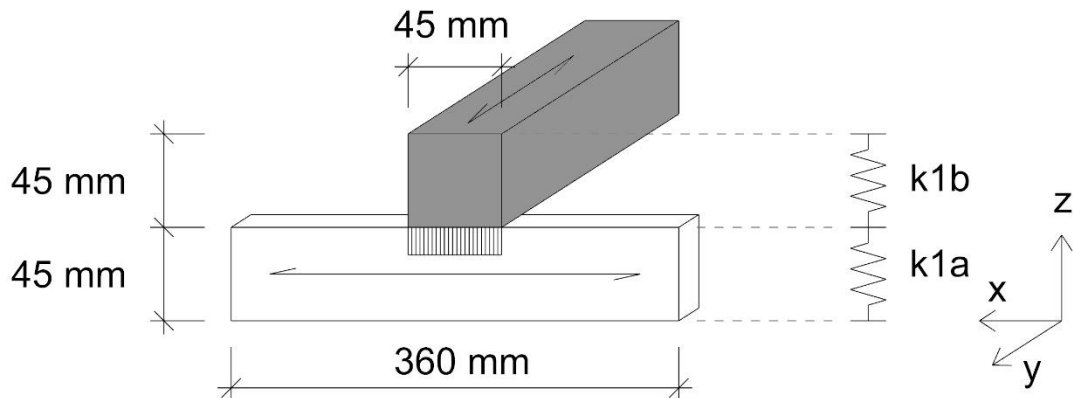


Figure 5.2 The superposition connection in the context.

For this connection analysis, the elements consist of timber with a rectangular cross section 45x45 mm, C24, with grain direction parallel to the “long” direction. The modulus of elasticity is 11000 MPa parallel to the grain and 370 MPa perpendicular to the grain. The shear modulus is 690 MPa and the density is 420 kg/m<sup>3</sup>. The connection zone is defined to be four times the element height, which can be seen in Figure 5.3, similar to the zone size defined by Nateghi, 1995.

### 5.2.1 Stiffness analysis

In order to assess the translational and rotational stiffness of the connection, the properties of the contact surfaces are examined. As an analytical approach, the elastic properties of the timber beams in contact are modelled as simple spring models, in a similar fashion as described by Descamps & Guerlement, 2009. The friction between the beams is neglected in these analytical calculations since it cannot be translated to a spring stiffness in the same way as the elasticity of the material. By assigning the correct modulus of elasticity to the right contact surface, the difference in material stiffness parallel and perpendicular to the grain is taken into account. The contact pressure that occurs between the supported beam, called “b”, and the supporting beam, called “a” when a translation is simulated in the negative z-direction is shown as a striped surface in Figure 5.3 below. “Beam b” is coloured in grey and sits on top of “Beam a”.



*Figure 5.3 Spring model for calculation of translation stiffness in the z-direction of the superposition connection. The direction of the grain is shown with arrows on the beams. “Beam b” in grey colour.*

For the superposition connection the translational and the rotational stiffness equals zero in all directions except one, translation in negative z-direction. This stiffness,  $Ct_z$ , is calculated by a simple spring model. The stiffness of a spring with modulus of elasticity  $E$ , cross sectional area  $A$  and length  $L$  is (Dahlblom & Olsson, 2010):

$$k = \frac{EA}{L} \quad (5.1)$$

Hence, the two springs in the model can each be calculated as:

$$k_{1a} = \frac{370 \cdot 10^6 \cdot 0.045^2}{0.045} = 16650 \text{ kN/m} \quad (5.2)$$

$$k_{1b} = \frac{370 \cdot 10^6 \cdot 0.045^2}{0.045} = 16650 \text{ kN/m} \quad (5.3)$$

Where  $k_{1a}$  is the stiffness induced by the supporting beam and  $k_{1b}$  is the stiffness induced by the supported beam. Since the springs are connected in series the total stiffness of the system,  $Ct_z$ , is calculated as:

$$Ct_z = \frac{1}{\frac{1}{k_{1a}} + \frac{1}{k_{1b}}} = \frac{1}{\frac{1}{16650} + \frac{1}{16650}} = 8325 \text{ kN/m} \quad (5.4)$$

## 5.3 Notched connection

The notched connection for this investigation is designed as a half lap joint with notches in both elements to be connected. The notches go down to half the height of the elements and this sets the eccentricity between the beams to zero, forming an entirely flat structure. Compared to the superposition connection this gives a structure where all the elements rest on the same level and the support relationship between the elements is hidden.

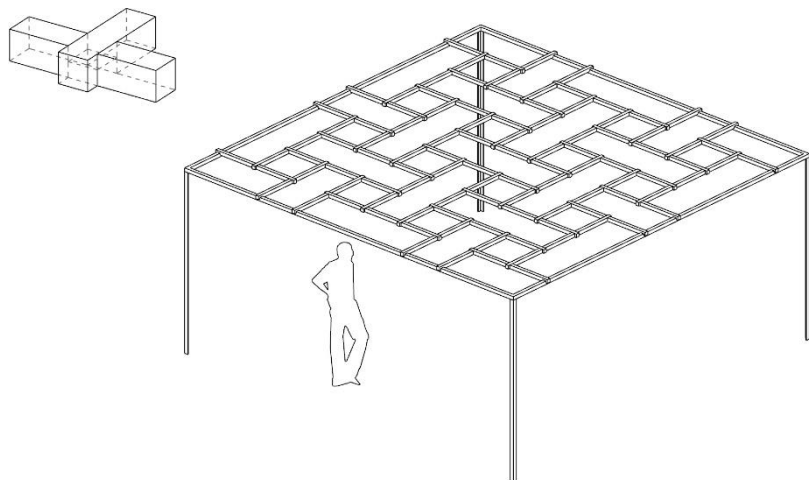
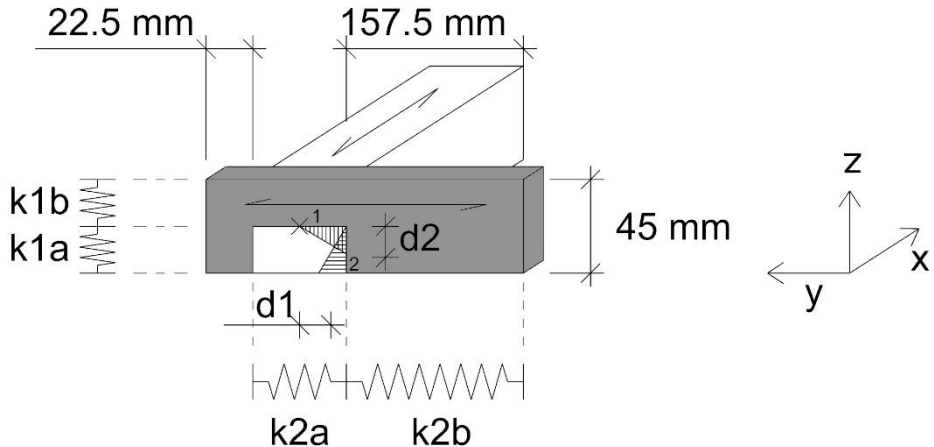


Figure 5.4 The notched connection in the context.

### 5.3.1 Stiffness analysis

The same timber, with the same material parameters and sizes as for the superposition connection is used for the notched alternative. Analytical calculations with spring models are used in the same way as described before to derive the translational,  $C_t$ , and rotational stiffnesses,  $C_r$ . As for the superposition connection, a connection zone of four times the height of the beam is defined. Hence, 157.5 mm of the elements on each side of the notch is included in the calculations, giving a length of 360 mm of the supporting beam. Since an example was given before on how to derive the translational stiffness, an example of how to calculate the rotational stiffness is given here. The fundamental principle is the same as for the translational stiffness calculations, namely to translate the materials in contact into spring models. The contact pressure that occurs when a rotation around the x-axis is simulated is shown as a striped area in Figure 5.5 below. The beam is assumed to rotate around the centre point of the notch, marked with a cross (X) in Figure 5.5.



*Figure 5.5 Spring model for calculation of rotational stiffness around the x-axis of the notched connection. The direction of the grain is shown with arrows on the beams. "Beam b" in grey colour.*

Rotation of the supported beam (shown in grey colour) around the x-axis will be restrained by the supporting beam at two contact surfaces. These are translated into four spring stiffnesses:  $k_{1a}$  for the first contact surface of the supporting beam,  $k_{1b}$  for the first contact surface of the supported beam,  $k_{2a}$  for the second contact surface of the supporting beam and  $k_{2b}$  for the second contact surface of the supported beam.

$$k_{1a} = \frac{370 \cdot 10^6 \cdot 0.0225 \cdot 0.045}{0.0225} = 16650 \text{ kN/m} \quad (5.5)$$

$$k_{1b} = \frac{370 \cdot 10^6 \cdot 0.0225 \cdot 0.045}{0.0225} = 16650 \text{ kN/m} \quad (5.6)$$

$$k_{2a} = \frac{370 \cdot 10^6 \cdot 0.0225 \cdot 0.045}{0.045} = 8325 \text{ kN/m} \quad (5.7)$$

$$k_{2b} = \frac{11000 \cdot 10^6 \cdot 0.0225 \cdot 0.045}{0.1575} = 70714 \text{ kN/m} \quad (5.8)$$

In order to calculate the rotational stiffness from these translational stiffnesses of each contact surface, a short derivation is necessary. If a bending moment  $M_x$  applied on the system results in a rotation angle  $\theta$  the rotational stiffness is:

$$Cr_x = \frac{M_x}{\theta} \quad (5.9)$$

The bending moment  $M_x$  in this case results in two compression forces,  $F_1$  and  $F_2$  acting on the beams (Descamps & Guerlement, 2009). These forces have the lever arms  $d_1$  and  $d_2$  respectively and hence,  $Cr_x$  can be rewritten as:

$$Cr_x = \frac{M_x}{\theta} = \frac{F_1 d_1 + F_2 d_2}{\theta} \quad (5.10)$$

Where:

$$d_1 = \frac{2}{3} \cdot 0.0225 = 0.015 \text{ m} \quad (5.11)$$

$$d_2 = \frac{2}{3} \cdot 0.0225 = 0.015 \text{ m} \quad (5.12)$$

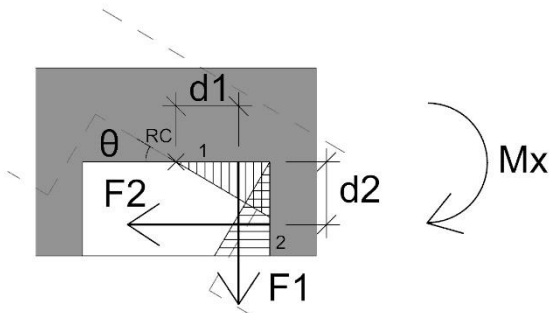


Figure 5.6 Definition of compression forces, lever arms and rotation angle induced by a bending moment.

The forces will cause a displacement  $\delta$  to occur in the materials. The force is proportional to the displacement and for the forces and stiffnesses in this case it can be written as:

$$F_1 = \delta_1 k_1 \quad (5.13)$$

$$F_2 = \delta_2 k_2 \quad (5.14)$$

It is assumed that only small rotations will occur in the joint. For small values on  $\theta$  the displacement can be approximated as:

$$\delta \approx \theta d \quad (5.15)$$

If this expression is inserted in equation (5.13) and (5.14) and then combined with equation (5.10) the equation below is obtained. In this equation  $\theta$  cancels out since it is included both in the numerator and denominator.

$$Cr_x = \frac{\delta_1 k_1 d_1 + \delta_2 k_2 d_2}{\theta} = \frac{\theta d_1 k_1 d_1 + \theta d_2 k_2 d_2}{\theta} = k_1 d_1^2 + k_2 d_2^2 \quad (5.16)$$

In the equations above,  $k_1$  and  $k_2$  are the total stiffness of contact surface 1 and 2. This means that  $k_{1a}$  and  $k_{1b}$  have to be converted into a total stiffness  $k_1$  before it is inserted in the equation. The same applies for  $k_{2a}$  and  $k_{2b}$  and is done in the same way as described before for equation (5.4).

$$k_1 = \frac{1}{\frac{1}{k_{1a}} + \frac{1}{k_{1b}}} = \frac{1}{\frac{1}{16650} + \frac{1}{16650}} = 8325 \text{ kN/m} \quad (5.17)$$

$$k_2 = \frac{1}{\frac{1}{k_{2a}} + \frac{1}{k_{2b}}} = \frac{1}{\frac{1}{8325} + \frac{1}{70714}} = 7448 \text{ kN/m} \quad (5.18)$$

When all the calculated parameters are inserted into equation (5.16) the rotational stiffness around the x-axis is obtained.

$$Cr_x = 8325 \cdot 10^3 \cdot 0.015^2 + 7448 \cdot 10^3 \cdot 0.015^2 = 3.55 \text{ kNm/rad} \quad (5.19)$$

In the same way, the rotational stiffnesses around the y- and z-axis are also calculated. The translational stiffnesses are calculated analogously to the example described for the superposition connection before. The stiffnesses are listed below and the following figures show the compression zones and spring models used in the calculations.

$$Ct_x = \frac{1}{\frac{1}{k_{1a}} + \frac{1}{k_{1b}}} = \frac{1}{\frac{1}{70714} + \frac{1}{8325}} = 7448 \text{ kN/m} \quad (5.20)$$

$$Ct_y = \frac{1}{\frac{1}{k_{1a}} + \frac{1}{k_{1b}}} = \frac{1}{\frac{1}{8325} + \frac{1}{70714}} = 7448 \text{ kN/m} \quad (5.21)$$

$$Ct_z = \frac{1}{\frac{1}{k_{1a}} + \frac{1}{k_{1b}}} = \frac{1}{\frac{1}{33300} + \frac{1}{33300}} = 16650 \text{ kN/m} \quad (5.22)$$

$$\begin{aligned} Cr_y &= k_1 d_1^2 + k_2 d_2^2 = \\ &= 8325 \cdot 10^3 \cdot 0.015^2 + 7448 \cdot 10^3 \cdot 0.015^2 = 3.55 \text{ kNm/rad} \end{aligned} \quad (5.23)$$

$$\begin{aligned} Cr_z &= k_1 d_1^2 + k_2 d_2^2 + k_3 d_3^2 + k_4 d_4^2 = \\ &= 3724 \cdot 10^3 \cdot 0.015^2 + 3724 \cdot 10^3 \cdot 0.015^2 + \\ &+ 4094 \cdot 10^3 \cdot 0.015^2 + 3724 \cdot 10^3 \cdot 0.015^2 = 3.43 \text{ kNm/rad} \end{aligned} \quad (5.24)$$

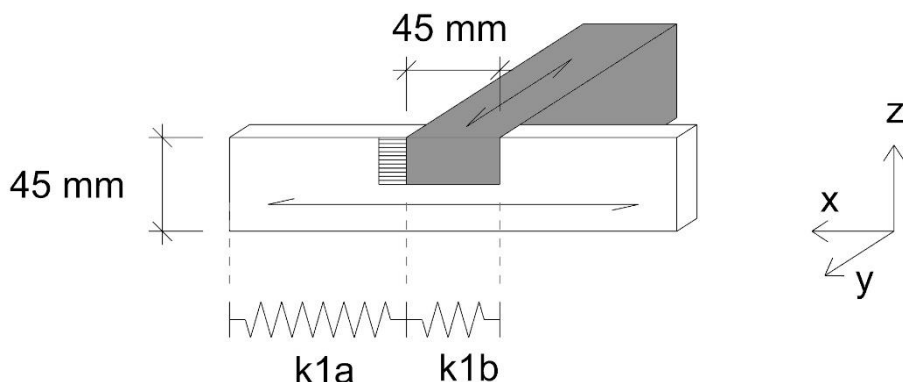


*Figure 5.7 Spring model for calculation of translational stiffness along the x-axis of the notched connection.*

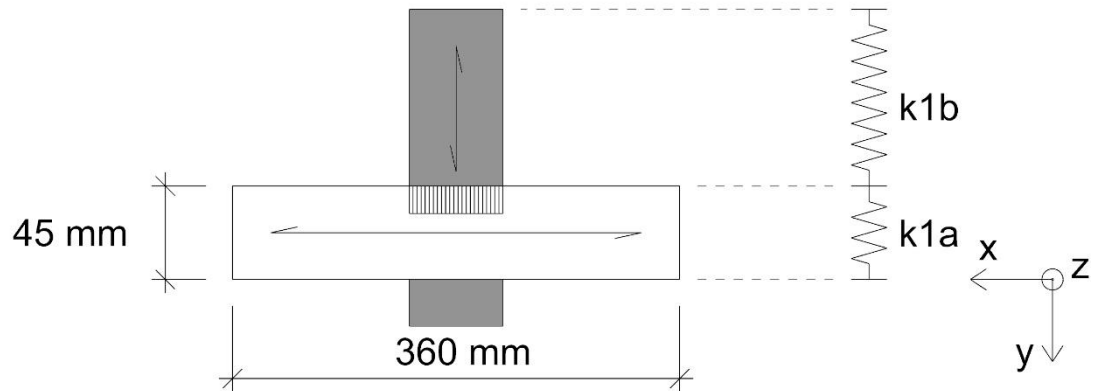


*Figure 5.8 Spring model for calculation of translational stiffness along the y-axis of the notched connection.*

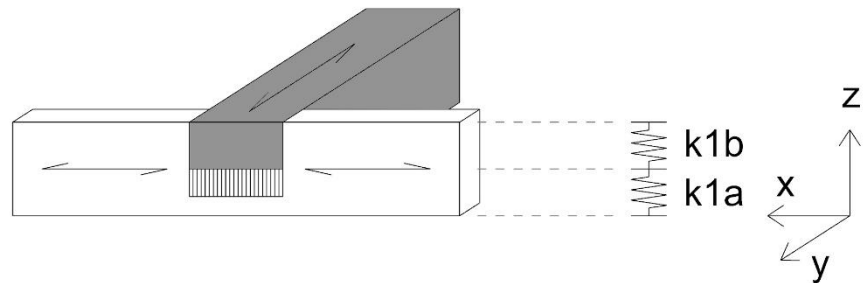


*Figure 5.9 Spring model for calculation of translational stiffness along the z-axis of the notched connection.*

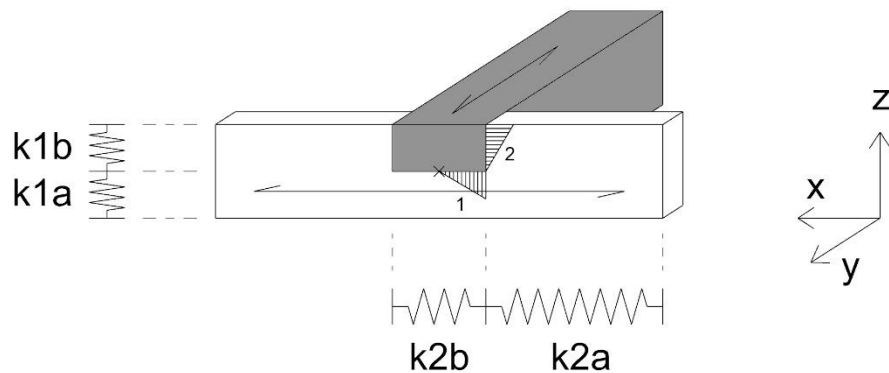


*Figure 5.10 Spring model for calculation of rotational stiffness around the y-axis of the notched connection.*

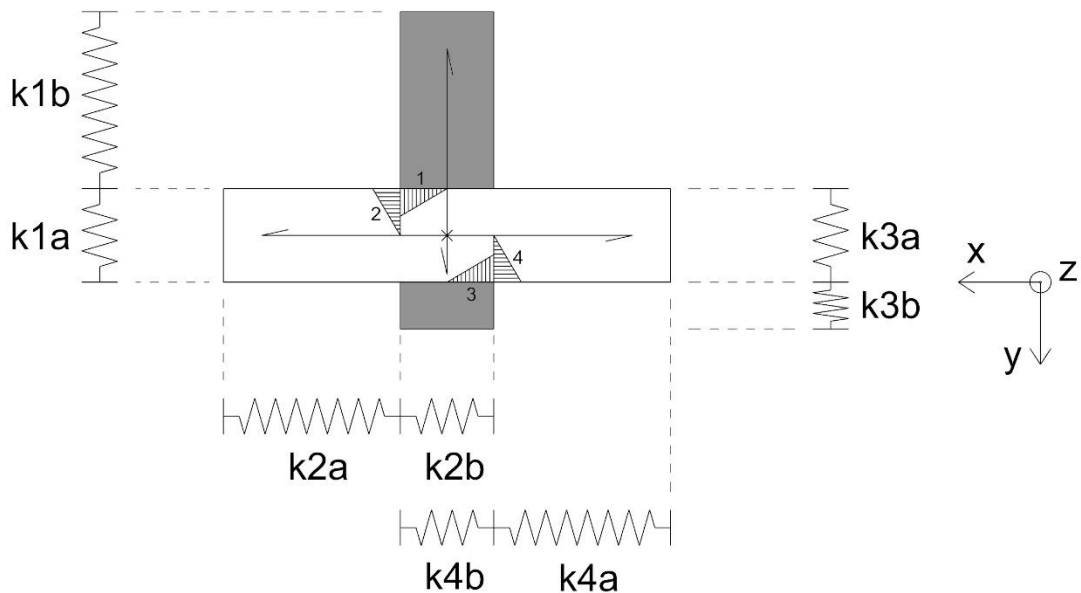


*Figure 5.11 Spring model for calculation of rotational stiffness around the z-axis of the notched connection.*

## 5.4 Global influence

Having the stiffness of the connections calculated, their influence on the global RF structure is analysed with the FEM software Karamba. Karamba is a tool linked to the CAD software Rhinoceros via the plug-in Grasshopper. In Grasshopper, a number of different components are connected with so called wires to build up a program with a desired function. Using Karamba for this investigation has the main advantage that it is adjustable to the CAD geometry created in Rhinoceros. In this way, calculations on different versions of the RF pattern can be tested without having to redefine the boundary conditions, loads etc. Also, the stiffnesses in the different axes can easily be adjusted to see how they influence different indicators, such as deflection, moments and shear force. The results are computed instantly as the parameters are changed and therefore their influence can be clearly understood.

### 5.4.1 The Karamba model

This chapter will describe how the model of the RF structure and its connections is built up in the FEM program Karamba. The Karamba model uses points from Rhinoceros to create the nodes of the model. To create the desired pattern, the points are placed at each intersection of the beams. When an alteration of the pattern should be tested, for example with larger engagement length, the points are simply moved to their new positions and the Karamba model will automatically be updated. The points can be seen to the left in the figure below and they are all assigned to a point parameter in Grasshopper.

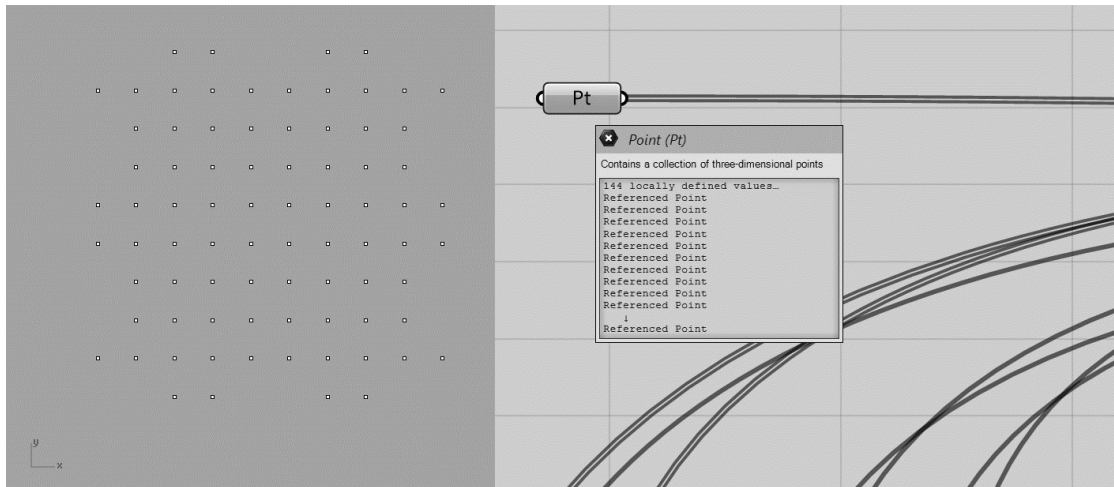


Figure 5.12 Input points from Rhinoceros to the left, assigned to a point parameter in Grasshopper.

As a next step, the points are assembled with Karamba's Assemble-component, creating an FE-model with node numbering. The node numbering can be seen in the figure below and one can note that there are quite a lot of nodes. This is because of duplicate nodes at all positions except the nodes at the perimeter. The node duplicates are there to create a small “column” at the joints, which is used as a concept to model the RF behaviour. This concept is described further later on.

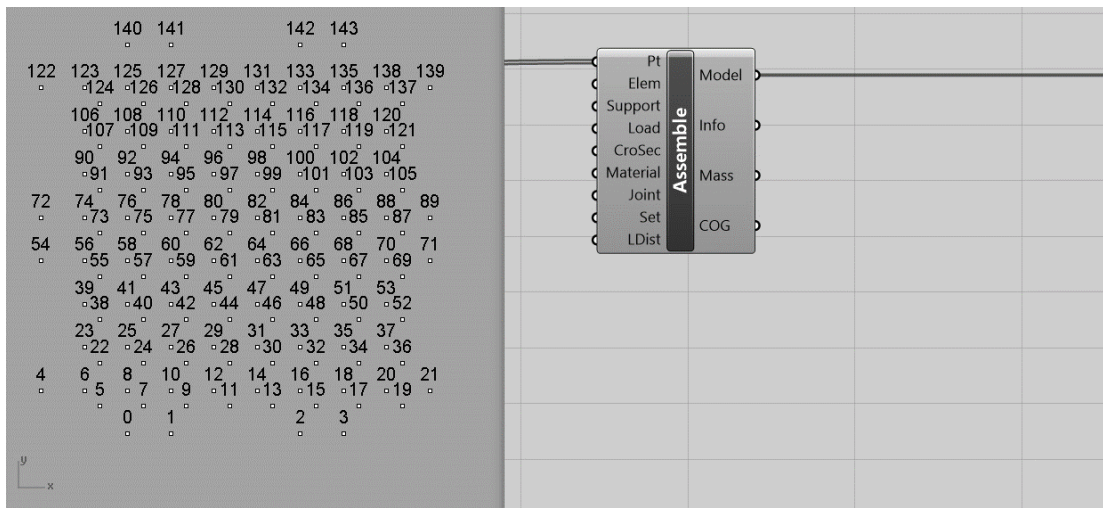
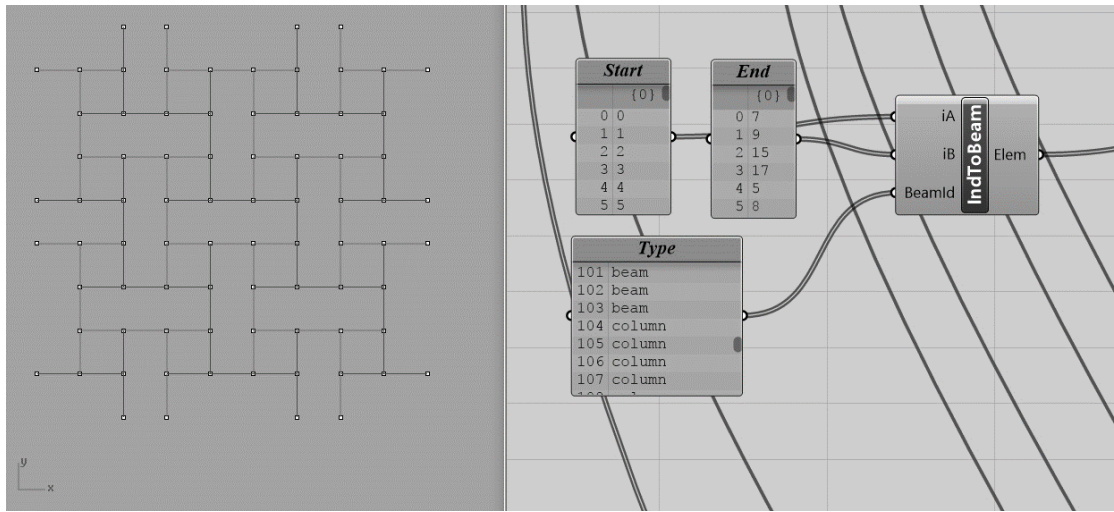


Figure 5.13 Node numbering created with the Assemble-component of Karamba.

Beam elements are defined between the nodes by using Karamba's IndToBeam-component. It creates a beam element between a start- and end-node and assigns a BeamId to it. The BeamId makes it possible to assign different cross sections and materials to the different beam types later on. Two beam types are created: One called “beam” which builds up the actual members of the RF, and another one called “column” which is used to model the joints.



*Figure 5.14 The IndToBeam-component which is used to create beam elements between the nodes.*

As mentioned earlier, a “column” is created at the points where two beams meet. It is defined as a beam element going between a lower and an upper node. This is a way of making it possible to adjust the stiffnesses of the joints and at the same time model the interlocking properties of the RF. In order to not have the “column” influencing the behaviour of the structure, it is made only 0.001 m high and infinitely stiff. More information about this is given when discussing cross sections and materials. In the figure below, the height of the column has been scaled up. For the RF fan including nodes 48,49,46,47,63,64,65 and 66 (located within the dashed lines in the figure below) the division between beam and column elements can be seen. The main advantage of this concept is that while for example node 63 can be assigned completely stiff properties (since it models a continuous beam), node 64 can have an adjustable stiffness to match the connection properties at the beam end.

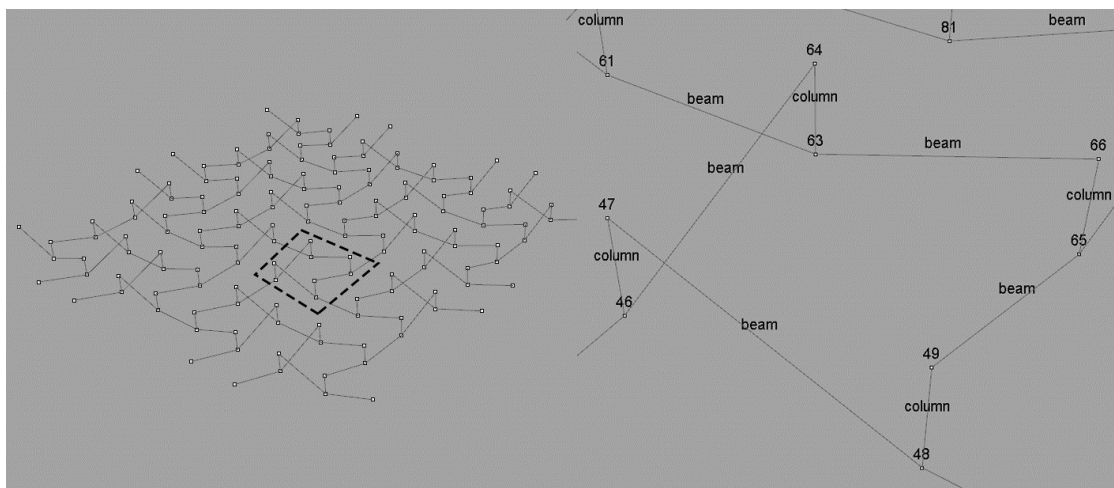


*Figure 5.15 Illustration of how the beams and columns are connected at the node duplicates. A zoomed in view on the beams within the dashed lines is shown to the right. The height of the columns are scaled up to make them visible.*

To input the connection stiffnesses into the model, the Beam-Joints-component is used. The Beam-joints are assigned to the columns and can be fed with translational and rotational stiffness for both the start and end-point of these elements. The starting point of a column is always placed at the bottom node, meaning that the columns go from the supporting beam to the supported beam with its endpoint in the top node. Therefore, to not give the continuous beams a local weakness, the value on Ct-start (kN/m) and Cr-start (kN/rad) is set to 1000000 which equals fully fixed. In contrast, for the end-stiffness, where two beams meet, the calculated values from the connection analysis is put in. In the figure below, the stiffness of the notched connection is shown. Note that for example the Ctz-stiffness is plugged in to the x-direction of the vector component due to transformation from local to global coordinate systems. The Beam-Joints component applies the stiffnesses to the local coordinate system of the column for which the x-axis equals the global z-axis. For the superposition connection, the stiffnesses that equals zero was put to 0.001 in order for the Karamba calculation to go through.

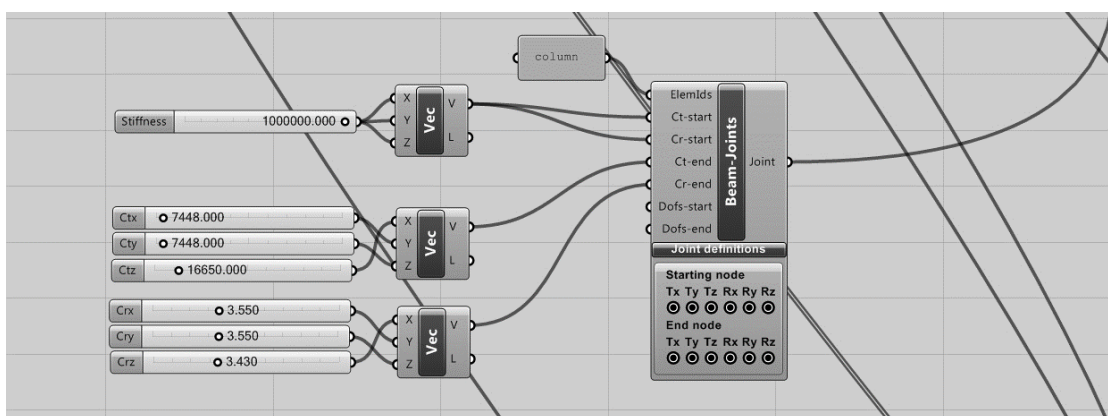


*Figure 5.16 The Beam-Joints-component is used to enter the stiffnesses derived from the calculations. In this case, the notched connection stiffness is shown.*

Next, information on the cross section and material of the beams is given by using the Cross Sections and MatSelect components. For both the beams of the structure and the “imaginary” columns a trapezoid cross section of 4.5x4.5 cm<sup>2</sup> is set. Since the default material library of Karamba does not contain timber of strength class C24, it is manually included by editing the material database. The modulus of elasticity is set to 11000 MPa, the shear modulus to 690 MPa and the specific weight is 4.124 kN/m<sup>3</sup>.

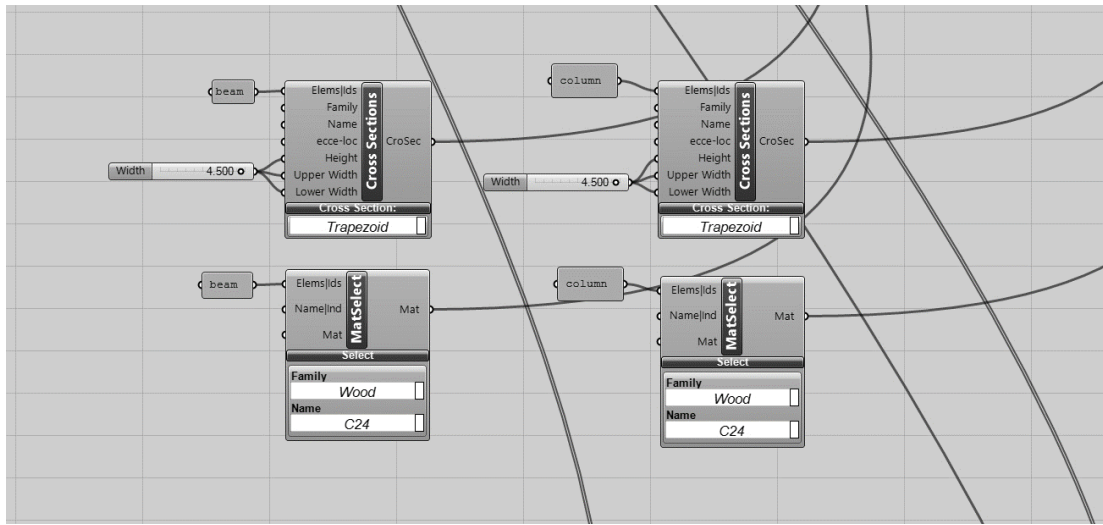


Figure 5.17 Assigning cross sectional and material properties to the beams and columns.

In order to sustain loads, the model needs to have supports defined at the nodes on the perimeter. They are applied by using the Support component and locking the translational degrees of freedom, Tx, Ty and Tz (seen as a black dot on the component). The structure is assumed to be pinned at the perimeter and hence the rotational degrees of freedom, Rx, Ry and Rz, are left free (no black dot). The node numbers where supports are placed can be read in the boxes in the figure below.

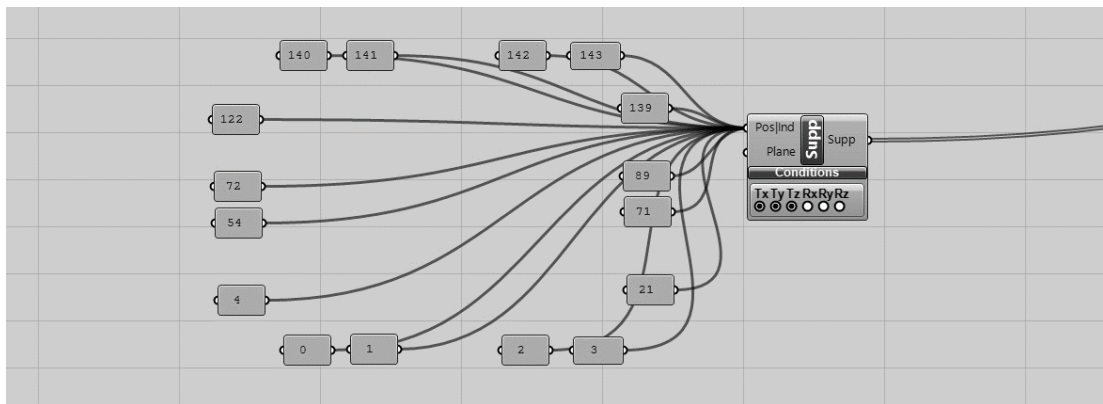


Figure 5.18 Pinned supports are assigned to the nodes on the perimeter. The node numbers can be read in the boxes which are placed in the same way as they appear in the structure.

Three different load cases are used in the investigation: Only self-weight of the beams (1), self-weight in combination with one point load (2) and self-weight in combination with two point loads (3). The first load case is created with the Loads component and a gravity load acting in negative z-direction. For load case 2 a point load of 0.25 kN in negative z-direction is added at node 78. Another point load is added to node 30 for the third load case, 0.25 kN in positive z-direction. The reason to why the load cases with point loads are included is to possibly amplify the results of the comparison of the connections.

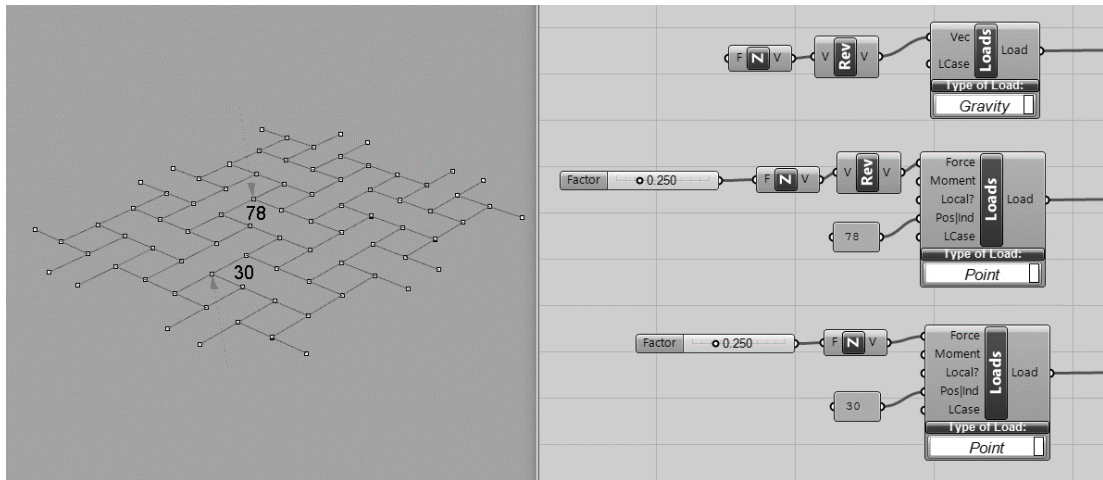


Figure 5.19 Definition of gravity load, one point load in negative  $z$ -direction at node 78 and another point load in positive  $z$ -direction at node 30.

To investigate if modification of the RF pattern, i.e. different engagement lengths, has any influence on the results, three different versions are tested: Engagement lengths of 0.555 m, 0.755 m and 0.355 m. Looking at the figure below, it is clear that the engagement length has quite a big influence on the appearance of the RF. The material needed to create the different versions of the pattern also varies. For engagement length 0.555 m the structure weighs 48 kg and the total beam length is 58 m. For 0.755 m the weight increases to 54 kg and the total length to 64 m. Among these three versions, 0.355 m engagement length gives the lowest weight and total length, 43 kg and 51 m. It can be concluded that the material use increases for increased engagement length.

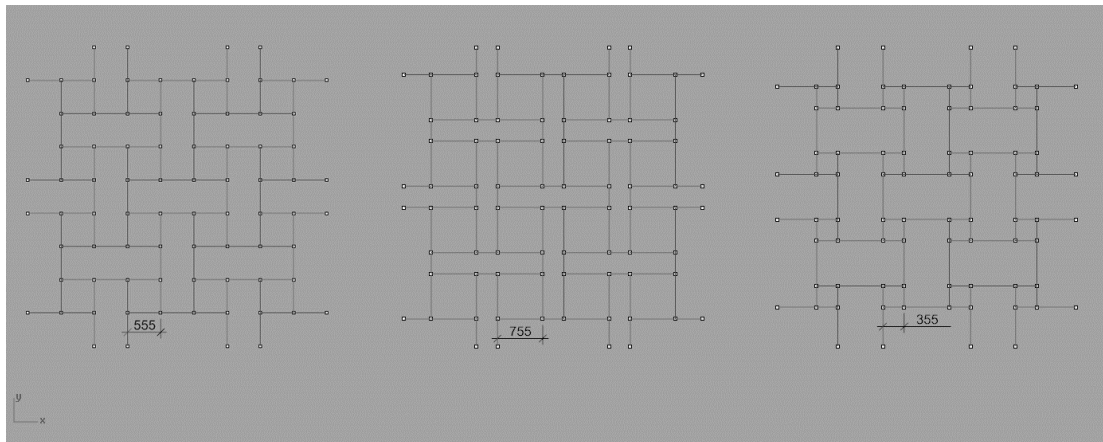


Figure 5.20 The three different engagement lengths included in the global analysis: 555 mm, 755 mm and 355 mm.

#### 5.4.1.1 Limitations

The Karamba model does not take the difference of the element shapes into account. The superposition elements have an S-shape with partly “double height” which makes the entire structure stiffer, while the notched elements are weaker due to the decreased cross section at the notches. Since the Karamba model only works with translational

and rotational stiffnesses at the nodes and homogenous  $45 \times 45 \text{ mm}^2$  timber as input, the different element stiffnesses of the superposition and notched elements is not included. On one hand, this could be seen as an important difference from reality but on the other hand it makes sense for the objective of this thesis: to compare the influence of the connection types. If the difference of element stiffness would be taken into account it would be more difficult to draw conclusions of what impact the connection properties have on the structure.

#### 5.4.1.2 Comparison with Abaqus

To verify the accuracy of the Karamba model, a global model of the RF has also been created in the FEM software Abaqus CAE, version 6-13. The beam parts, in this case the elements of the notched connection, are created by importing CAD geometry in ACIS-format. Elastic material properties are used with the type “Engineering constants” where E1, E2, E3, Nu12, Nu13, Nu23, G12, G13 and G23 can be adjusted. For beams orientated along the x-axis E1 is set to 11000 MPa while E2 and E3 both are set to 370 MPa. For beams orientated along the y-axis, E2 is set to 11000 MPa and E1 and E3 are 370 MPa. This is to take the grain direction into account. The Poisson’s ratios, the Nu-values, are all set to 0.04 and the shear modulus is 690 MPa. To model the connection between the beams, interactions are created at all intersections. The interactions include a normal behaviour with “Hard” contact. A gravity load of  $9.81 \text{ m/s}^2$  is defined in negative z-direction and acts on every element. On the perimeter, a Displacement/Rotation boundary condition with fixed translations but free rotations is applied to the end surfaces of the beams. For the global seeds of the model, an approximate size of 0.01125 is used.

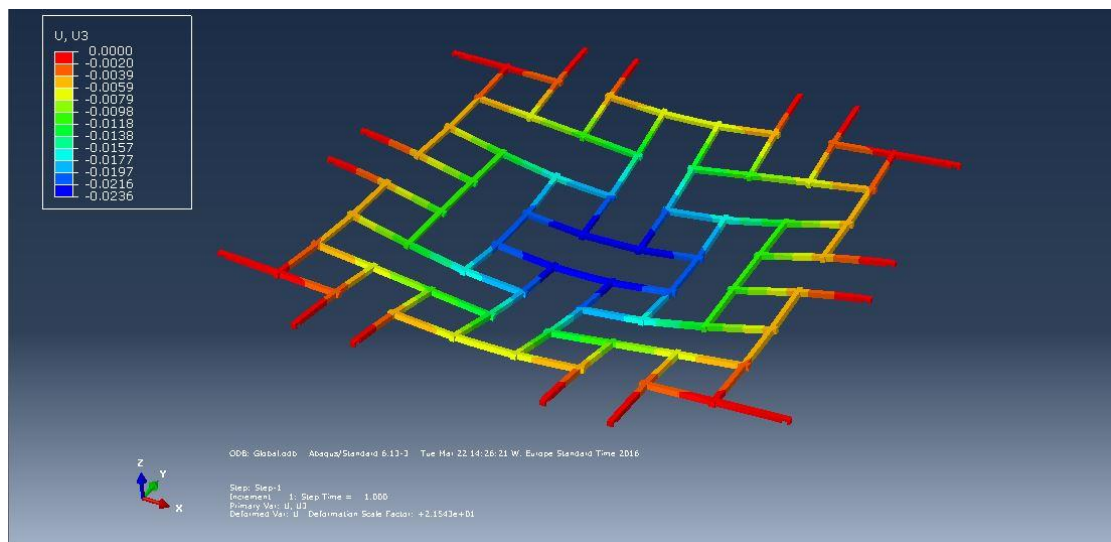


*Figure 5.21 Deflected structure obtained from Abaqus. Maximum deflection is 0.0236 m. The deflection is scaled up to make it more visible and the numbers in the legend are given in m.*

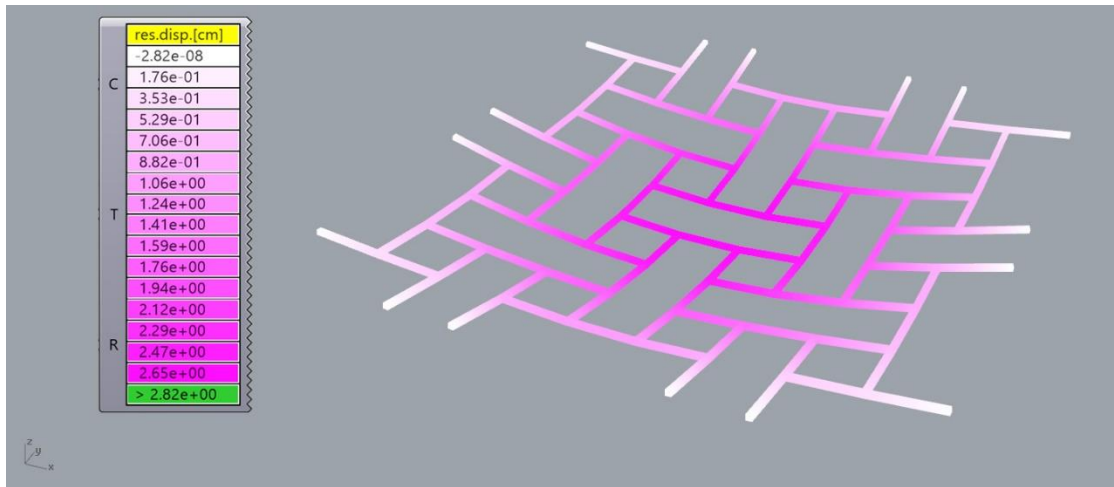


*Figure 5.22 Deflected structure obtained from Karamba. Maximum deflection is 0.0296 m. The deflection is scaled up to make it more visible. The numbers in the legend are given in cm.*

Although the structure shows similar deflection pattern in the two programs, it can be concluded that there is a small difference between the maximum displacements. With the notched connection stiffness, the maximum deflection obtained from Karamba is 0.0296 m while Abaqus calculates it to 0.0236 m. The result from Karamba is 25% higher than the Abaqus-result. Based on the fact that the two models show somewhat similar results, the Karamba model is assumed to have enough accuracy for the main objective of this thesis – to compare the influence of the connections.

## 5.4.2 Results

In this section, the results of the calculations on the global structure are presented. The connections have been inserted in several alterations of the RF pattern, each with different engagement lengths. Also, the connections have been tested for different combinations of loads. For description of each load case, see chapter 5.4.1.

### 5.4.2.1 Deflection

Looking at the maximum deflection of the structure, it can be concluded that the superposition connection contributes to a higher deflection than if the notch design is applied to the joints. This is true for all the load cases and engagement lengths. Also, the larger engagement length of the pattern, the larger the difference between the two connections. For the pattern with engagement length 755 mm the relative displacement is larger than for a pattern with shorter engagement length. In addition, for both the superposition and notched connection the deflection decreases for decreased engagement length.

*Table 5.1 Maximum deflection of the structure.*

Loadcase	Engagement length [m]	Superposition [m]	Notched [m]	Comparison [%]	Comparison [mm]
1	555	0.0303	0.0286	6%	2
	755	0.0337	0.0314	7%	2
	355	0.0272	0.0261	4%	1
2	555	0.0650	0.0604	8%	5
	755	0.0689	0.0625	10%	6
	355	0.0630	0.0591	7%	4
3	555	0.0486	0.0441	10%	5
	755	0.0511	0.0454	13%	6
	355	0.0477	0.0439	9%	4

#### 5.4.2.2 Bending moment

The maximum bending moment about the local y-axis of the elements follows more or less the same pattern as the deflection: The superposition connection generates a higher bending moment in the beams than the notched connection. As for the deflection, the bending moment decreases for decreased engagement length.

*Table 5.2 Maximum bending moment in the structure.*

Loadcase	Engagement length [m]	Superposition [kNm]	Notched [kNm]	Comparison [%]	Comparison [Nm]
1	555	0.0465	0.0435	7%	3
	755	0.0538	0.0493	9%	5
	355	0.0398	0.0380	5%	2
2	555	0.1863	0.1676	11%	19
	755	0.2041	0.1812	13%	23
	355	0.1676	0.1518	10%	16
3	555	0.1638	0.1460	12%	18
	755	0.1737	0.1533	13%	20
	355	0.1510	0.1353	12%	16

#### 5.4.2.3 Torsional moment

According to the calculations, having connections with only superposition generates zero torsional moment in the beams. This is reasonable since there is no rotational stiffness in these connections that can transport such a force in the structure. For the notched joint, there are some torsional moment in the structure, measuring between 2 and 12 Nm for the different patterns and load cases. As for the deflection and the bending moment, the torsional moment decreases for decreased engagement length.

The comparison in percentage has been left out in the result table because the torsional moment equals zero for all the superposition-cases.

*Table 5.3 Maximum torsional moment in the structure.*

Loadcase	Engagement length [m]	Superposition [kNm]	Notched [kNm]	Comparison [%]	Comparison [Nm]
1	555	0.0000	0.0029		3
	755	0.0000	0.0037		4
	355	0.0000	0.0024		2
2	555	0.0000	0.0076		8
	755	0.0000	0.0117		12
	355	0.0000	0.0061		6
3	555	0.0000	0.0068		7
	755	0.0000	0.0101		10
	355	0.0000	0.0051		5

#### 5.4.2.4 Shear force

Similar to the deflection and bending moments, the shear force is larger for the superposition connection than the notched connection. But in contrast to the other indicators, the shear forces increases for decreased engagement length.

*Table 5.4 Maximum shear force in the structure.*

Loadcase	Engagement length [m]	Superposition [kN]	Notched [kN]	Comparison [%]	Comparison [N]
1	555	0.0845	0.0791	7%	5
	755	0.0728	0.0677	8%	5
	355	0.1113	0.1050	6%	6
2	555	0.3354	0.3116	8%	24
	755	0.2700	0.2520	7%	18
	355	0.4721	0.4344	9%	38
3	555	0.2949	0.2706	9%	24
	755	0.2298	0.2127	8%	17
	355	0.4253	0.3848	11%	41

#### 5.4.2.5 General conclusions

When compared, the indicators behave in approximately the same way and give somewhat the same relative results for the different patterns and load cases. The deflection, bending moment, torsional moment and shear force are all 2-13% larger for the superposition connection compared to the notched connection. The first three

indicators all decrease for decreased engagement length, while the shear force increases for decreased engagement length.

## 6 Structural design

In order to assess the theoretical viability of the notched connection, a structural design of a RF is carried out. From the loads acting on the structure, a certain force pattern is created, partly depending on the properties of the connections. The aim of the structural design is to verify that the members are able to carry these forces.

### 6.1 Context and indata

As defined for the investigation in the previous chapter, the context for this RF is also a roof structure spanning 5x5 m (more exactly 4995x4995mm in order to suit the RF pattern), possibly for an exhibition stand, see Figure 5.4. The notched connection type is chosen for the design, mainly to investigate its major issue regarding decreased cross section at the notches, but also because of promising properties for this type of structure, such as speed of construction. The structure is assumed to be simply supported on the outer edge, i.e. free rotations but locked translations. For all the beams in the structure the following solid timber material properties is used:

Strength class: C24

Bending strength parallel to grain:  $f_{m,k} = 24 \text{ MPa}$

Shear strength:  $f_{v,k} = 4.0 \text{ MPa}$

Elastic modulus parallel to grain:  $E_{0,mean} = 11000 \text{ MPa}$

Shear modulus:  $G_{mean} = 690 \text{ MPa}$

Density:  $\rho_{mean} = 420 \text{ kg/m}^3$

### 6.2 Design procedure

To design the RF, the initial step is to calculate the loads. These loads will then be entered in Karamba where the effects on maximum deflection  $w$ , bending moment  $M_{Ed}$ , torsional moment  $T_{Ed}$  and shear force  $V_{Ed}$  will be calculated. Next, deflection limits  $w_{inst}$ ,  $w_{fin}$  and the capacities of a certain cross sectional size will be calculated,  $M_{Rd}$ ,  $T_{Rd}$ ,  $V_{Rd}$ ,  $V_{Rd,notch}$  (the reduced capacity at the notch). The parametric property of Karamba makes it possible to instantly see how the adjustment of the cross sectional sizes affects the design moments and forces. In that way the width and height of the members can easily be changed to see when the capacity exceeds the load effects. A number of initial test calculations showed that the deflection requirement was often the hardest indicator to achieve and hence it is tested first in the design procedure. When a sufficient cross section for the deflection requirement is found, all the other capacities are checked. In case of concluding that the cross section is not enough for any of these indicators, a new cross section is tested. The design procedure is summarized in the list below.

- Define the loads.

- Calculate cross section to fulfil deflection requirement  $w_{inst}$  and  $w_{fin}$ .
- Calculate design moments and forces  $M_{Ed}$ ,  $T_{Ed}$  and  $V_{Ed}$ .
- Check capacities  $M_{Rd}$ ,  $T_{Rd}$ ,  $V_{Rd}$  and  $V_{Rd,notch}$ .
- Choose a final cross section.

### 6.2.1 Loads

Apart from the self-weight of the structure, point loads of 0.02 kN are assumed to affect the structure at each node except the nodes on the outer edge where the structure is supported. These point loads represent installations, for example lamps, that could be attached to the roof structure of an exhibition stand. This means that the load combination according to Eurocode 1 consists of one self-weight of the structure,  $G_1$ , and one permanent load of the installations,  $G_2$ . For checking maximum deflection, the Quasi-permanent load combination for Serviceability Limit State (SLS) is used. For this load combination the safety factor for permanent loads equals 1.0 which gives:

$$G_1 + G_2 \quad (6.1)$$

The self-weight and the load of the installations are added in Karamba using the load component where the load types Gravity and Point are chosen respectively. The gravity load in Karamba is a function of the size of the member and therefore it automatically adjusts as the cross section is changed. For a cross section of 95x45mm the total weight of the structure is 101.8 kg.

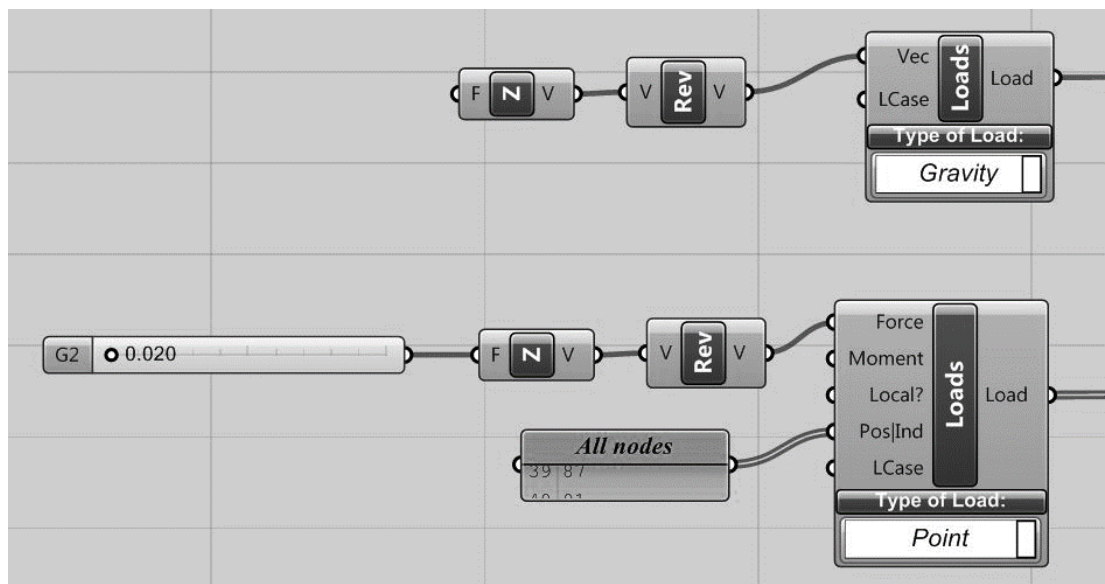


*Figure 6.1 Definition of gravity and point load in Karamba to represent the SLS load combination of permanent loads.*

When calculating the design load effects on bending moment, torsion and shear force, the fundamental load combination for the Ultimate Limit State (ULS) is used. The

partial safety factor  $\gamma$  is 1.35 for both the self-weight and the point loads. In Karamba, the safety factors are applied as factors to the load component for the gravity and point load.

$$1.35 \cdot G_1 + 1.35 \cdot G_2 \quad (6.2)$$

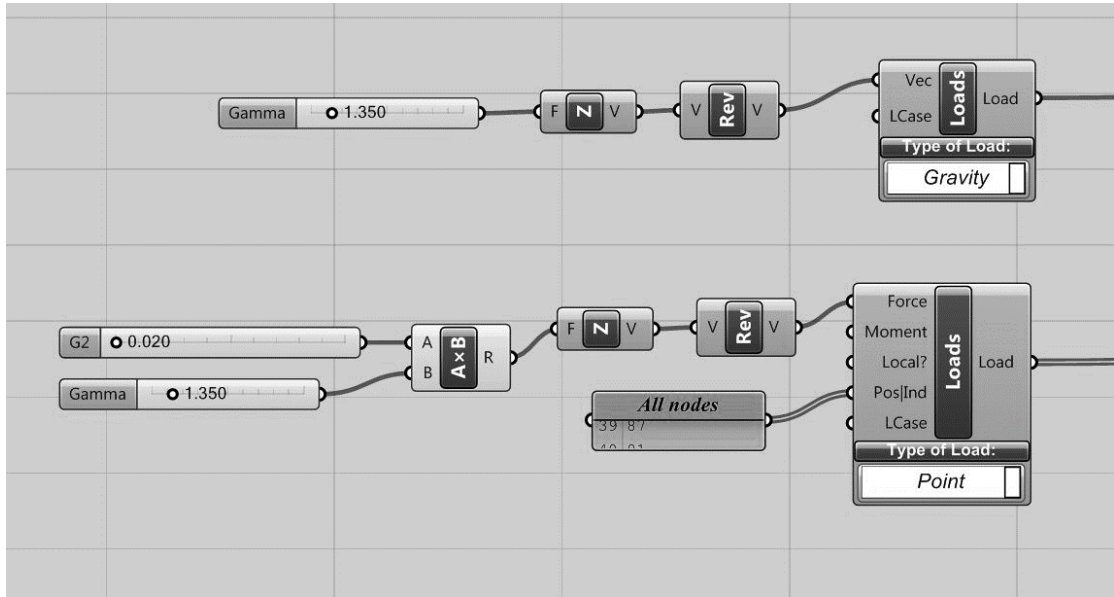


Figure 6.2 Definition of gravity and point load in Karamba to represent the ULS load combination of permanent loads.

### 6.2.2 Achieving deflection requirement

Eurocode defines limits for the deflection, one for the instant deflection  $w_{inst}$  and one for final deflection  $w_{fin}$  which takes the effect of creep into account. The two limits for deflection of the structure are calculated below.

$$w_{inst} = \frac{L}{300} = \frac{4.995}{300} = 0.0167 \text{ m} \quad (6.3)$$

$$w_{fin} = \frac{L}{150} = \frac{4.995}{150} = 0.0333 \text{ m} \quad (6.4)$$

Assigning the SLS load combination to Karamba according to Figure 6.1, the deflection requirements are met for a cross section with height of 95mm and width of 45mm. This value was reached by setting the width to 45mm and then increasing the height until the deflection requirements were fulfilled. The calculated instant deflections for this cross section, caused by the self-weight, point loads and both loads, are stated below.

$$w_{inst,G1} = 0.0070 \text{ m} \quad (6.5)$$

$$w_{inst,G2} = 0.0097 \text{ m} \quad (6.6)$$

$$w_{inst} = w_{inst,G1} + w_{inst,G2} = 0.0070 + 0.0097 = 0.0167 \text{ m} \quad (6.7)$$

To calculate the final deflection, the influence of creep has to be included and this is made with the factor  $k_{def}$  according to Eurocode 5. This factor depends on the climate class of the structure which in this case is assumed to be 1, corresponding to an indoor environment. This results in  $k_{def} = 0.6$ . From the initial deflection obtained from Karamba, the final deflection is calculated below.

$$w_{fin,G1} = w_{inst,G1} (1 + k_{def}) = 0.0070 \cdot (1 + 0.6) = 0.0112 \text{ m} \quad (6.8)$$

$$w_{fin,G2} = w_{inst,G2} (1 + k_{def}) = 0.0097 \cdot (1 + 0.6) = 0.0155 \text{ m} \quad (6.9)$$

$$w_{fin} = w_{fin,G1} + w_{fin,G2} = 0.0112 + 0.0155 = 0.0267 \text{ m} \quad (6.10)$$

### 6.2.3 Design moments and forces

After the deflections requirements are fulfilled, the design bending moment, torsional moment and shear force for this cross section can be obtained from Karamba. In these calculations the ULS load combination is used in Karamba according to Figure 6.2. The design load effects are listed below and will later be used to check the capacity of the cross section.

$$M_{Ed} = 0.3084 \text{ kNm} \quad (6.11)$$

$$T_{Ed} = 0.0064 \text{ kNm} \quad (6.12)$$

$$V_{Ed} = 0.5606 \text{ kN} \quad (6.13)$$

### 6.2.4 Check of capacities

#### 6.2.4.1 Bending moment capacity

The design bending moment capacity  $M_{Rd}$  is calculated by using Navier's formula. Since there is no normal force in the members it cancels out in the equation. Similar to how a design elastic modulus was calculated for the deflection check, a design bending strength needs to be calculated before input in the equation for moment capacity. In addition to the partial factor, this also involves the factor  $k_{mod}$  which takes load duration into account. For this structure a medium term load duration is assumed which generates a  $k_{mod}$  of 0.8. Also, Eurocode 5 states that solid timber members with height less than 150 mm can have their bending strength increased by a factor  $k_h$  which is calculated below. Since the moment, and all the other capacities, is checked at the notch, half of the beam height is used,  $h_{ef}$ . The variable  $I$  below is the moment of inertia for the rectangular cross section. After the capacity is calculated it is compared to the design moment calculated above.

$$k_h = \min \left\{ \left( \frac{150}{h_{ef}} \right)^{0.2}, \frac{1.2586}{1.3} \right\} = \min \left\{ \left( \frac{150}{47.5} \right)^{0.2}, \frac{1.2586}{1.3} \right\} = \min \left\{ 1.2586, 1.2586 \right\} = 1.2586 \quad (6.14)$$

$$f_{m,d} = k_h k_{\text{mod}} \frac{f_{m,k}}{\gamma_M} = 1.2586 \cdot 0.8 \frac{24}{1.3} = 18.5886 \text{ MPa} \quad (6.15)$$

$$I = \frac{bh_{ef}^3}{12} = \frac{0.045 \cdot 0.0475^3}{12} = 4.0189 \cdot 10^{-7} \text{ m}^4 \quad (6.16)$$

$$M_{Rd} = \frac{2 \cdot f_{m,d} I}{h_{ef}} = \frac{2 \cdot 18.5886 \cdot 10^6 \cdot 4.0189 \cdot 10^{-6}}{0.0475} = 0.3145 \text{ kNm} \quad (6.17)$$

$$M_{Rd} = 0.3145 \text{ kNm} > M_{Ed} = 0.3084 \text{ kNm} \Rightarrow \text{OK!} \quad (6.18)$$

#### 6.2.4.2 Torsional moment capacity

To calculate the design torsional moment capacity  $T_{Ed}$  the shear strength needs to be reduced with safety factors analogous to previous calculations. In addition to that, Eurocode includes a factor  $k_{shape}$  when calculating the torsional capacity, which takes the cross sectional shape into account. The variable  $J$  in the calculations below is the polar moment of inertia. The radius of the cross section is the diagonal from the centerpoint and out to the outer edge. In the final step it is checked against the design torsional moment.

$$k_{shape} = \min \begin{cases} 1 + 0.15 \cdot \frac{h_{ef}}{b} \\ 2.0 \end{cases} = \min \begin{cases} 1 + 0.15 \cdot \frac{0.0475}{0.045} \\ 2.0 \end{cases} = \min \begin{cases} 1.1583 \\ 2.0 \end{cases} = 1.1583 \quad (6.19)$$

$$f_{v,d} = k_{\text{mod}} \frac{f_{v,k}}{\gamma_M} = 0.8 \frac{4}{1.3} = 2.4615 \text{ MPa} \quad (6.20)$$

$$J = 0.23 \cdot h_{ef} b^3 = 0.23 \cdot 0.0475 \cdot 0.045^3 = 9.9554 \cdot 10^{-7} \text{ m}^4 \quad (6.21)$$

$$r = \sqrt{\left(\frac{b}{2}\right)^2 + \left(\frac{h_{ef}}{2}\right)^2} = \sqrt{\left(\frac{0.045}{2}\right)^2 + \left(\frac{0.0475}{2}\right)^2} = 0.0327 \text{ m} \quad (6.22)$$

$$T_{Rd} = \frac{k_{shape} f_{v,d} J}{r} = \frac{1.1583 \cdot 2.4615 \cdot 10^6 \cdot 9.9554 \cdot 10^{-7}}{0.0327} = 0.0868 \text{ kNm} \quad (6.23)$$

$$T_{Rd} = 0.0868 \text{ kNm} > T_{Ed} = 0.0064 \text{ kNm} \Rightarrow \text{OK!} \quad (6.24)$$

#### 6.2.4.3 Shear force capacity

The shear force capacity is calculated by using Jourawski's formula. The same design shear strength as calculated above is used and the capacity is checked against the design shear force. But Eurocode also states that a reduction factor with regard to existing cracks in the member should be applied, namely  $k_{cr}$ .

$$k_{cr} = \min \begin{cases} \frac{3}{f_{v,k}} = \min \begin{cases} \frac{3}{4} = 0.75 \\ 1 \end{cases} \\ 1 \end{cases} \quad (6.25)$$

$$V_{Rd} = \frac{2 \cdot f_{v,d} k_{cr} b h_{ef}}{3} = \frac{2 \cdot 2.4615 \cdot 10^6 \cdot 0.75 \cdot 0.045 \cdot 0.0475}{3} = 2.6307 \text{kN} \quad (6.26)$$

$$V_{Rd} = 2.6307 \text{kN} > V_{Ed} = 0.5606 \text{kN} \Rightarrow \text{OK!} \quad (6.27)$$

#### 6.2.4.4 Shear force capacity at notch

Since there is a risk for high stress concentrations at the notches of the beams, Eurocode 5 states that the shear capacity should be checked for a reduced depth  $h_{ef}$ , in this case half of the beam height. Below, the capacity that is needed at the notch is calculated and compared with the design shear force. The calculation includes a reduction factor  $k_v$  which takes the shape of the notch into account. Apart from the height of the member,  $k_v$  also depends on the variables  $k_n$ ,  $i$ ,  $\alpha$  and  $x$  which are all calculated below for the particular notch in this structure. The variable  $x$  is the distance from support reaction force to the corner of the notch and in this case it is assumed to equal half of the beam width.  $k_{cr}$  is applied in these calculations as well.

$$\text{Solid Timber} \Rightarrow k_n = 5 \quad (6.28)$$

$$90 \text{ degree angle of the notch} \Rightarrow i = 0 \quad (6.29)$$

$$\alpha = \frac{h_{ef}}{h} = \frac{0.0475}{0.095} = 0.5 \quad (6.30)$$

$$x = \frac{b}{2} = \frac{45}{2} = 22.5 \text{mm} \quad (6.31)$$

$$k_v = \min \begin{cases} 1 \\ \frac{k_n \left( 1 + \frac{1.1 \cdot i^{1.5}}{\sqrt{h}} \right)}{\sqrt{h} \left( \sqrt{\alpha(1-\alpha)} + 0.8 \frac{x}{h} \sqrt{\frac{1}{\alpha} - \alpha^2} \right)} = \end{cases} \quad (6.32)$$

$$= \min \begin{cases} 1 \\ \frac{5 \cdot \left( 1 + \frac{1.1 \cdot 0^{1.5}}{\sqrt{95}} \right)}{\sqrt{95} \left( \sqrt{0.5 \cdot (1-0.5)} + 0.8 \frac{22.5}{95} \sqrt{\frac{1}{0.5} - 0.5^2} \right)} = \min \begin{cases} 1 \\ 0.6834 \end{cases} = 0.6834 \end{cases}$$

$$V_{Rd,notch} = \frac{k_v f_{v,d} k_{cr} b h_{ef}}{1.5} = \frac{0.6834 \cdot 2.4615 \cdot 10^6 \cdot 0.75 \cdot 0.045 \cdot 0.0475}{1.5} = 1.7979 \text{ kN}$$
(6.33)

$$V_{Rd,notch} = 1.7979 \text{ kN} > V_{Ed} = 0.5606 \text{ kN} \Rightarrow \text{OK!}$$
(6.34)

### 6.2.5 Final design

The cross section with height 95 mm and width 45 mm have been proved to pass all the checks above. Except for the bending moment capacity, it can be noted that the checks for the capacity in ULS pass with quite a big margin. The utilization ratios are calculated below.

$$\frac{M_{Rd}}{M_{Ed}} = \frac{0.3084}{0.3145} = 98\%$$
(6.35)

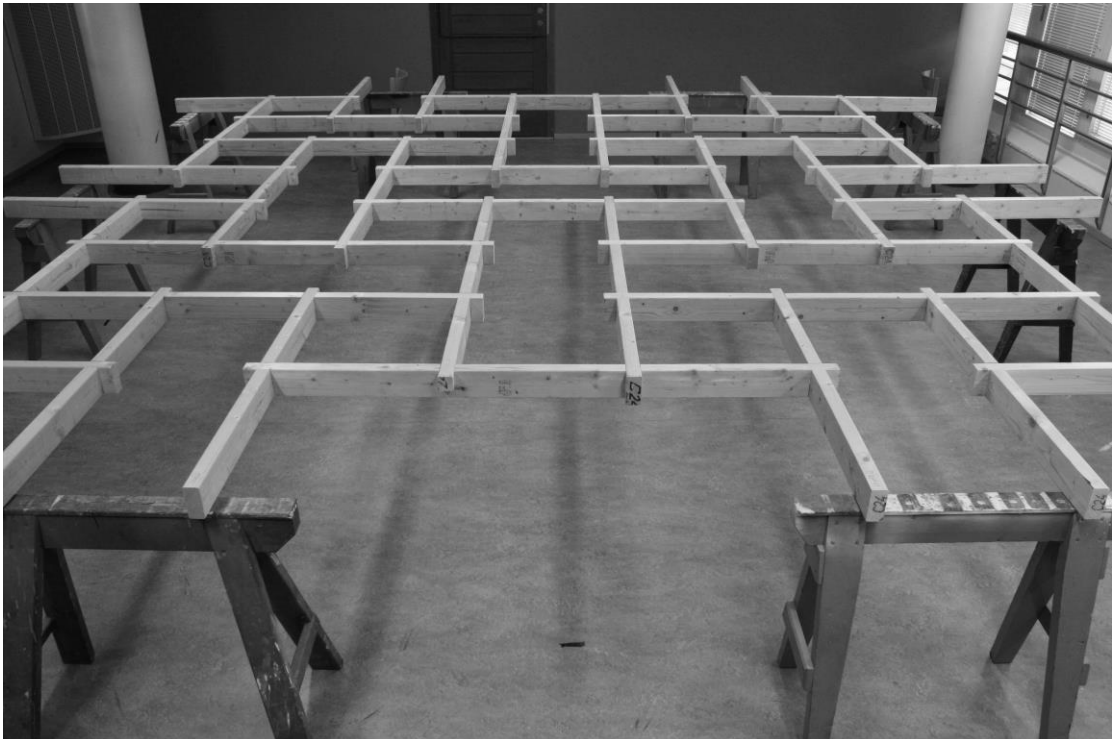
$$\frac{T_{Rd}}{T_{Ed}} = \frac{0.0063}{0.0868} = 7\%$$
(6.36)

$$\frac{V_{Rd}}{V_{Ed}} = \frac{0.5606}{2.6308} = 21\%$$
(6.37)

$$\frac{V_{Rd,notch}}{V_{Ed}} = \frac{0.5606}{1.7979} = 31\%$$
(6.38)

## 7 Physical model

In the final phase of this project, a full scale physical model was built in order to ensure the feasibility of the notched connection and the RF. This model was also tested to see if the behaviour corresponded to the calculations. The same span (5x5 m<sup>2</sup>) and beam dimensions (45x95 mm<sup>2</sup>) were used as in the sizing calculations described in the previous chapter.



*Assembled full size physical model. The span between the trestles is 5x5 m.*

### 7.1 Material

The wood was bought from Beijer Byggmaterial, a timber shop in Gothenburg. According to Beijer, the moisture content of the 45x95 mm C24 fir timber beams is 16% and the density is 460 kg/m<sup>3</sup>. Since this density is higher than the one used in the calculations (420 kg/m<sup>3</sup>), the material properties in Karamba was updated to enable comparison between test results and the FE model.

Previous chapters have indicated that a benefit from using RFs is that the short elements are easy to transport. To investigate this, the timber was brought from the timber shop to the test site on Chalmers University of Technology using only public transportation. The timber was cut to the beam lengths (1794 mm for long elements and 1275 mm for shorter edge elements) directly in the timber shop to be able to fit into a bus. For bus transfers a trolley was used to carry the beams.



*Figure 7.1 The beams were cut to shorter lengths in the timber shop to be able to bring on public transportation buses. A trolley was used at bus transfers.*

The 40 beams of the structure were carried in 5 packages containing 8 beams each. One package weighed approximately 30 kg and it was only convenient for one person to transport one package at a time. This meant that one person needed to go back and forth between the timber shop five times to fetch all the material.

## 7.2 Production of notches

With the beams transported to Chalmers University of Technology, the production of the notches took place in the wood workshop at the Department of Architecture. To create the notches a circular saw was used with a blade width of 3 mm. By making several cuts with the blade at the node position, a 47.5 mm deep (half of the beam height 95 mm) and 45 mm wide notch was created. The distance from the beginning of the outer notch and the edge of the beam was made 42 mm.



*Figure 7.2 Producing a notch in a circular saw by cutting away more and more material.*

### 7.3 Assembly

The RF was assembled by one person on top of 750 mm high trestles. First, the beams were laid out on the floor in the pattern of the structure, without being connected to each other. Then one of the central fans was created by connecting three beams and inserting the fourth in an angle and rotating it in place. Getting the fourth beam in place was a bit difficult since no margin had intentionally been created for the lap joints while producing the beams. The beam needed to be pushed quite hard to fit into the fan. When the fan was formed, four trestles were placed to support the beams on their outer edge. This procedure was then repeated for the other elements of the structure, where every third beam needed to be rotated in place. Pictures of the complete assembly are shown in Figure 7.5.

Rotating the beams in place involved lifting another element, which due to the nature of the RF caused lifting of all the other elements. Lifting the element while getting the other beam in place was no problem for one person to do for these beam dimensions, even though the weight increased as the structure grew. But the lifting created stresses on other elements which caused the end of one beam to crack and fall off during the assembly. This can be seen in Figure 7.3 below. Since this end part of the beam does not contribute to the strength of the structure against vertical loads this element was not repaired or replaced.



*Figure 7.3 End part of one beam cracked during assembly.*

It was stated above that no margin intentionally was left in the notches to ease the assembly. However, due to inaccuracy of the cutting, some notches were a bit wider than 45 mm, hence creating a gap in the connection and the structural influence of this will be discussed later on. A connection with a gap is shown in Figure 7.4.

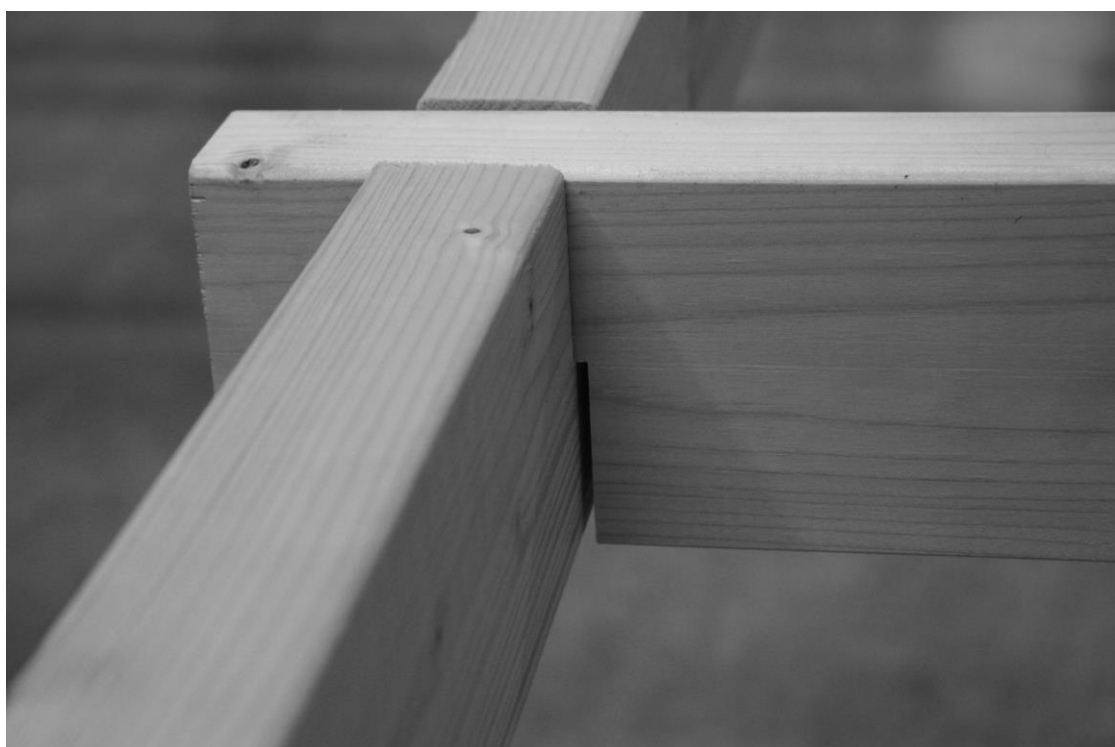


*Figure 7.4 Gap in a connection due to inaccurate cutting.*

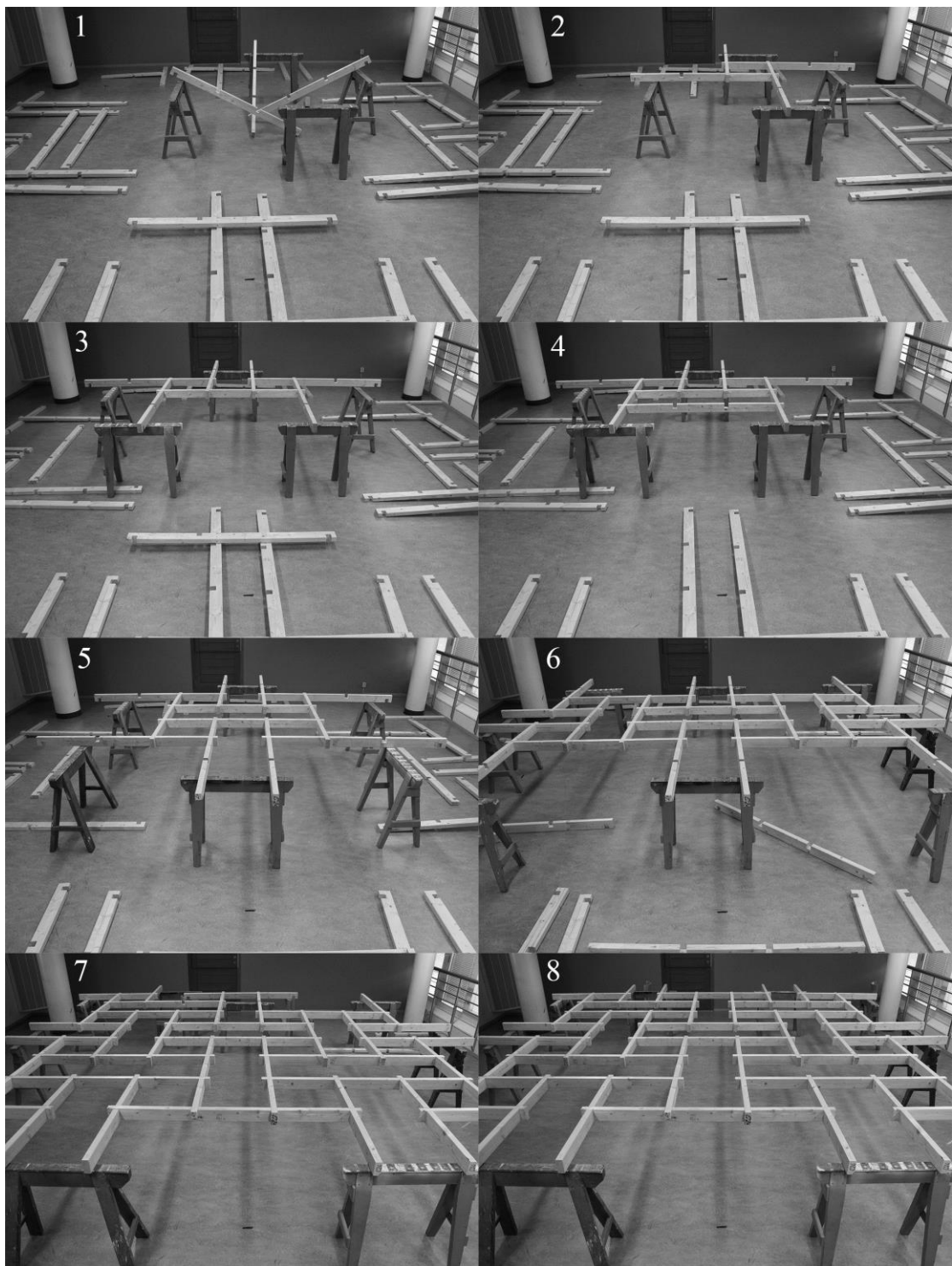


Figure 7.5 Complete assembly of the RF.

## 7.4 SLS load test

In the previous chapter, the beams were sized to carry a SLS load consisting of the structure's self-weight and installations hung to the connections. These "installation loads" were applied to the physical model and the deflection was measured for comparison with calculated values.

### 7.4.1 Test setup

After the assembly of the structure deflection gauges were installed at two of the four inner nodes. The precision of the gauges was 0.01 mm. One gauge was placed with a 45 mm offset in one direction from a node and the other gauge with 45 mm offset in the other direction from another node in order to make room for hanging lead weights to the nodes, as can be seen in the figure below. The weights were tied to the nodes using thin ropes and weighed approximately 2 kg each to correspond to the 0.020 kN load used in the calculations.



*Figure 7.6 The SLS test setup with lead weights applied to all connections and deflection gauges installed.*

Figure 7.7 below shows the node numbers of the joints where 2 kg lead weights were applied. The weights were first applied to the node row going from number 5 to 19 and the deflection was read on the gauges. This procedure was then repeated for the node rows 22-36, 38-52, 55-69, 73-87, 91-105, 107-121, 124-137 until all nodes were loaded. The labels G1 and G2 mark where the gauges were placed on the structure.

124	126	128	130	132	134	136	137	
107	109	111	113	115	117	119		121
91	93	95	97	99	101	103		105
73	75	77	79	81	83	85	87	
55	57	59	61	63	65	67	69	
38	40	42	44	46	48	50		52
22	24	26	28	30	32	34		36
5	7	9	11	13	15	17	19	

Figure 7.7 Node numbers to which 2 kg lead weights were applied. G1 and G2 shows the position of the two deflection gauges.

#### 7.4.2 Results

In the table below, the deflection caused by the loading of each node row is given. The deflection called  $w_{mean}$  is the mean value of the deflection read on the two gauges ( $w_1$  and  $w_2$ ) and  $w_{calc}$  is the deflection derived for the corresponding load in Karamba. The comparison is the ratio between  $w_{mean}$  and  $w_{calc}$  and it can be concluded that the measured deflection and the calculated deflection differ quite much. For load applied to all nodes (5-137) the measured deflection was 30 mm while the calculated deflection was 10 mm.

*Table 7.1 Results of the SLS load test*

Node row	$w_1$ [mm]	$w_2$ [mm]	$w_{mean}$ [mm]	$w_{calc}$ [mm]	comparison [-]
5-19	1.78	1.36	1.57	0.64	245%
22-36	5.16	4.05	4.61	1.79	257%
38-52	10.18	8.08	9.13	3.52	259%
55-69	15.58	13.45	14.52	5.38	270%
73-87	25.66	18.49	22.08	6.99	316%
91-105	25.19	23.93	24.56	8.32	295%
107-121	28.32	27.80	28.06	9.21	305%
124-137	30.02	29.91	29.97	9.66	310%

## 7.5 Failure load test

After the structure had been tested for deflection due to SLS loads the structure was loaded until failure. This was yet another way of evaluating the FE model by comparing it to the response of the physical model, but also a way to observe the failure mode.

### 7.5.1 Test setup

The four inner nodes, number 61, 63, 79 and 81, had their lead weights replaced by baskets while the 2 kg weights remained on all the other nodes. In this way, weights could easily be added into the baskets and the deflection read for each step. However, due to the length of the deflection gauges, the deflection could only be read until 72.3 mm, which took place when 41 kg was applied to each of the four nodes. The gauges were placed in the same positions as for the previous test.



*Figure 7.8 Setup for failure load test. Baskets hung to the four inner nodes and 2 kg lead weights remaining on the rest.*

When 65 kg had been applied to each of the four nodes the test had to be paused and continued 24 hours later. With 70 kg applied, there was no more room for weights in the baskets or to tie them to the node and therefore a pallet was put on top of the centre nodes. It is assumed that the load applied on top of the pallet is distributed evenly to the four nodes. The pallet was loaded until 92 kg stressed each node and at that point two bigger lead weights of 45.5 kg and 44.7 kg were placed on it which caused failure of the structure.

## 7.5.2 Results

### 7.5.2.1 Deflection

In the first table below, the deflection due to the first load applications in the baskets is shown. Applied weight is the mean value of the total weight applied to the four inner nodes (not including the 2 kg weights applied to the rest of the nodes). The first applied load is the weight of the baskets and at this point the deflection gauges were cleared and consequently the deflection is zero.  $w_{mean}$  is the mean value of the deflections read on the two gauges, but G2 ran out of length at 44 mm deflection so from that point the deflection was only read on G1.

It is worth mentioning that the structure was left for 16 hours with the SLS load applied. Since the gauges were left on the structure the creep deflection could be measured to 5.4 mm. As the load was applied successively to the structure it was also noted that the gauge pointers never settled on a value but continued to increase. The deflection was read as quickly as possible after each loading but since it took some time to gather the weights for the next load application, the creep influenced all

measurements. The speed of the gauge pointers, i.e. the speed of the creep, increased as the load increased.

*Table 7.2 Deflection during the failure load test*

Applied weight [kg]	$w_{mean}$ [mm]	$w_{calc}$ [mm]	Comparison [-]
2.73	0	-	-
7.62	8.44	13.20	64%
12.28	17.01	16.15	105%
16.93	26.19	19.10	137%
21.55	33.91	22.02	154%
26.52	43.89	25.17	174%
30.06	50.60	27.41	185%
34.84	60.15	30.44	198%
39.65	69.70	33.49	208%
41.11	72.80	34.41	212%

### 7.5.2.2 Failure load and failure mode

When the structure failed, 114.37 kg was applied to each of the four mid nodes (in total 4x114.37 kg plus 2 kg applied to all of the other nodes). However, the structure failed directly when the last load, weighing 44.7 kg was applied and thus the failure load could also be lower. The load level before 114.37 kg was 103.19 kg which means the failure load was somewhere between these values.

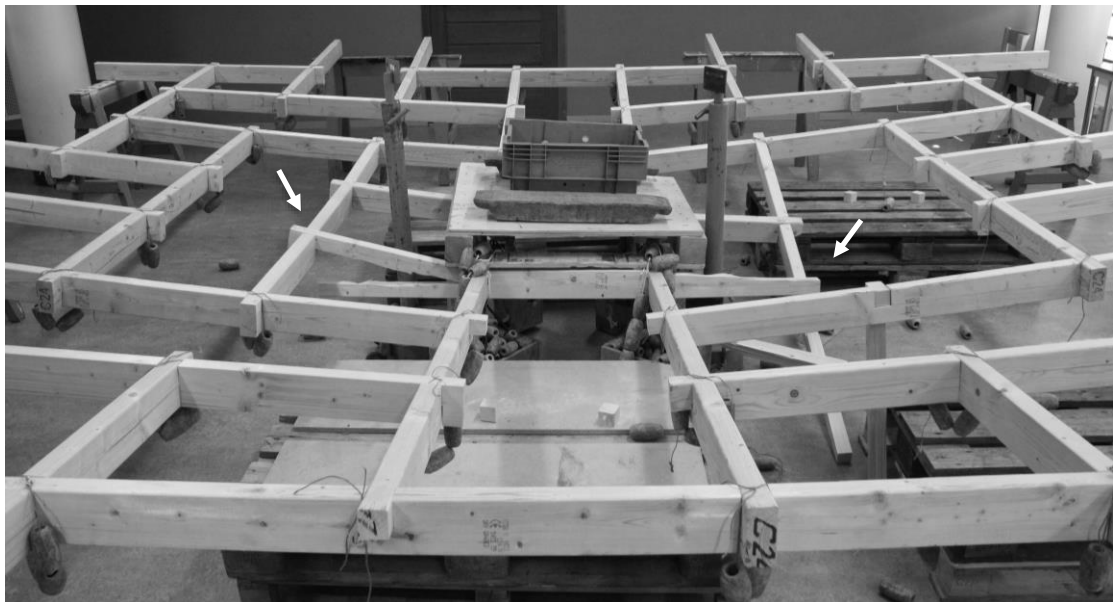


*Figure 7.9 The failure load test setup after the failure. After the baskets were full, a pallet was put on top of the structure as a platform for additional loads. The last load to be applied was the big lead weights seen closest to the camera. The arrows indicate possible starting positions of the failure.*

The failure was very brittle without major visible cracks or cracking sounds. It started in the supported end of one element (marked with white arrows in the figure above), as a crack parallel to the grain at the top corner of a notch. This crack then quickly spread from the outer notch to the inner notch where another element was supported. This behaviour clearly indicates a shear failure mode due to stress concentrations at the notches. The starting position of the crack is in line with the FE model since it calculates the maximum shear force at these points (node 59, 65, 77 and 83). In Figure 7.10 below, a zoomed in view of the two elements that failed is shown. The top beam in the figure spanned between node 59 and 65 while the bottom beam spanned between node 48 and 101.

According to the FE model, the failure mode would be in bending with 160 kg applied to the four nodes if the full height of the cross section (95 mm) could be utilized. If only half of the height could be utilized (47.5 mm) due to the notch, the structure was calculated to fail in bending for only 26 kg. But, as stated above, the failure occurred due to shear splitting at the notch and the calculated failure load for that scenario was 265 kg (to each of the four nodes), utilizing half the height. With the safety factor  $k_s$  applied the calculated value for shear splitting decreased to 175 kg.

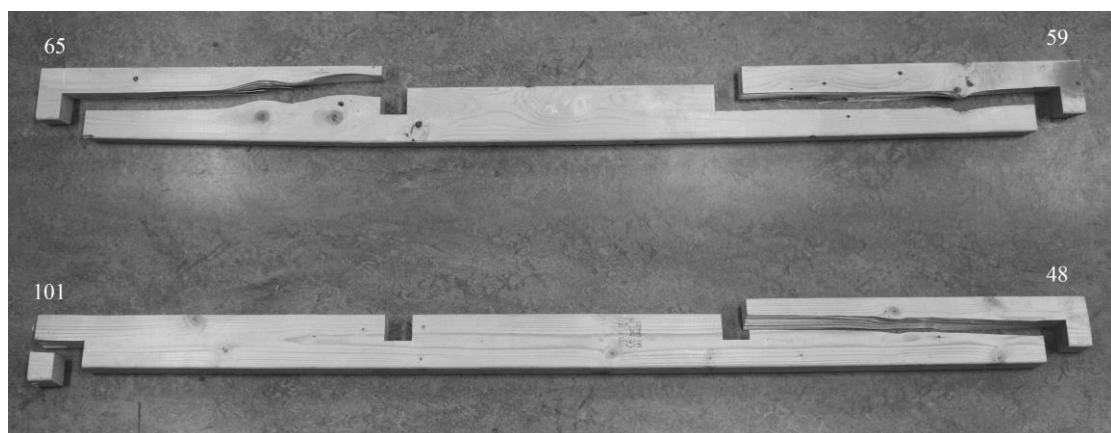


*Figure 7.10 The two beams that failed during the test. The numbers indicate the position of the nodes.*

When the structure failed, one of the beams fell down on two of the baskets which started to act as supports. This is the state of the failed structure above. Since the baskets prevented increased deflection, failure at more nodes was probably avoided. However, a property of a RF with this kind of notched connection is that the structure can still transfer loads even if some elements have failed, thanks to formation of new load paths. This was tested in the physical model by removing the baskets and all other weights. In the figure below, the structure successfully carries its self-weight even though the two broken beams have been removed. This would not have been possible with a superposition connection.

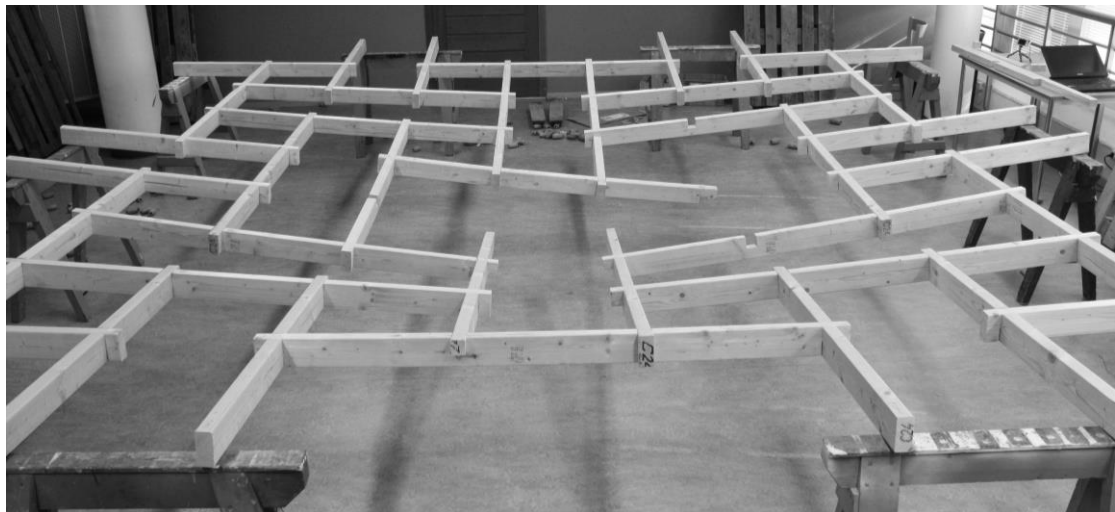


*Figure 7.11 The structure successfully carrying its self-weight even when two beams have failed and been removed.*

## 8 Discussion

This chapter discusses the results obtained in the key chapters of this thesis: Connection types, Connection analysis, Structural design and Physical model.

### 8.1 Connection types

From the literature study made during this thesis, four main connection types were defined: Superposition, Couplers, Dowels and plates and Notches. This classification is quite similar to existing ones and was assessed as a good enough basis for the connection evaluation. Thönnissen (2015) presents another classification which is perhaps more clear and suitable to reciprocal frames: *Contact bearing*, *Addition* and *Subtraction*, where the first corresponds to a Superposition connection (elements simply in contact), the second to Couplers, Dowels and plates (where something needs to be added) and the third to Notches (where material is subtracted).

The evaluation of the connection types in this thesis is to a large extent based on sources dealing with timber connections in general, not with focus on applications in RFs. Perhaps the most rewarding section of the evaluation is the built examples presented for each connection type. In that section the connection properties become more visible and measurable. Without a context it is difficult to with certainty assess what influence a connection type has, since it can be adjusted to the project to some extent. Hence, it is suggested for future investigations on connections in RFs to directly implement them in a specific context as was done first in Chapter 5 in this thesis. From that point they can all be evaluated further with regard to production, assembly, appearance and structural properties.

### 8.2 Connection analysis

The first section of the connection analysis derived the translational and rotational stiffness of one superposition and one notched connection. The calculations were based on the geometry and material properties of these specific connections and the results can therefore certainly not be seen as very general. Another factor influencing the result is the size of the connection zone, i.e. how much of the beam that is included in the spring stiffness. The influence of altering the geometry, material and connection zone has not been assessed in this thesis, but would of course be a relevant study to perform. The connection stiffness has only been derived with analytical calculations. To verify the accuracy of these calculations, numerical and experimental analyses should also be performed.

What influence the connections have on the structural behaviour of a certain RF was assessed in the second section of this chapter. The investigations made in Karamba did only consider the stiffness of the connections, not the geometry and stiffness of the beam which is also highly dependent on the chosen connection. For example, the beam with notches and the S-shaped beam for the superposition connection clearly have different stiffness properties that will influence the structural behaviour. However, neglecting the stiffness of the elements lead to a study completely linked to the connection stiffness.

For the comparison between the Karamba model and a model made in Abaqus, it is worth mentioning that the support conditions of the latter was probably too stiff. The

translational degrees of freedom were locked in every direction for the entire end surface of each beam on the boundary. Doing this resulted in a fixed boundary condition for the Abaqus model while the Karamba beams are simply supported. However, because of the notches located very close to the supports in Abaqus, the beams are quite flexible in this region and this could be a reason to why the results of the two software are still similar.

### 8.3 Structural design

As discussed for the connection analysis above, the stiffness was only derived for a specific beam cross section. The result of the structural design was a cross section with twice the height of this cross section (45x45 mm compared to 45x95 mm). Of course a stiffness analysis of the larger cross section will lead to another stiffness which in turn will affect the result of the structural design. This impact has not been assessed in detail but the comparison between the structural influence of the superposition and notched connection indicates that a less stiff connection gives higher deflection, bending moment and shear force.

The structural design was only carried out for a notched connection and for a certain composition and RF pattern which of course limits its generality. However, it definitely points out important aspects to consider when designing an RF, such as fulfilling the deflection requirements and what capacities to check. It also presented a convenient way of combining load effect calculations in Karamba with analytical checks of the capacities.

### 8.4 Physical model

Carrying the material from the timber shop was quite heavy, but still fully possible, for one person to do alone, especially if another transportation than a public bus is used. Assembling the structure was surprisingly easy and with movable temporary supports this could be done in a convenient way on a building site, most probably also for even larger beams.

The physical model deflected much more than what was expected from the calculations, 30 mm instead of 10 mm, and there are a number of possible reasons to this:

- The unintended gaps in the connections, due to inaccurate cutting, was not included in the calculations but it is possible that they increased the deflection of the physical model.
- The material of the physical model could have had weaker strength properties than the ones used in the calculations. The theoretical material properties are the lower 5% of strength values derived in experiments, meaning that there is a 5% risk that the physical model had weaker material than what was used in the calculations.
- The stiffness of the element is not accurately modelled in Karamba where the elements are simplified as straight elements without the notches.

Loading the structure until failure resulted in a different failure mode and failure load than what the calculations showed. Instead of failing in bending for 160 kg, the

structure failed in shear due to notch effect for 114 kg. In addition to the reasons stated above, the following could be added as possible explanations:

- For large deflections, non-linear behaviour can occur and cause a change in force distribution in the system. This second order effect has not been accounted for in the FE model.
- The safety factor  $k_v$ , accounting for notch effect in Eurocode 5, is highly dependent on the material properties and it is obvious that it cannot be attributed to all soft wood materials.

To prevent this kind of shear failure, the members can be strengthened in a number of ways, for example by a screw perpendicular to the grain. However, this will have an impact on the appearance which will have to be taken into account. It should also be noted that this happened when loading the structure until failure and not with SLS loads applied.

## **9 Conclusion**

### **9.1 Background**

***How has reciprocity been used for load bearing structures throughout history?***

The earliest use of reciprocity as a structural principle has been traced to bridges in Asia 900 years ago. During the Middle Ages it was used in floor structures as a solution to lack of beams of sufficient length. Built examples from the 20<sup>th</sup> century and today show applications in roof structures and temporary pavilions.

***What are the main parameters defining a RF?***

The main parameters are the style of the fan, the number of elements in the assembly, the eccentricity, the engagement length, the element length and the composition of members in the structure.

***What element types and composition types can be identified?***

The main element types can be categorized in elongated, plate, ring and combined elements. A composition can be either flat or curved.

***What connection types can be used in timber RF structures?***

Superposition, Couplers, Dowels and Notches.

### **9.2 Evaluation**

***How can the connection be produced?***

Superposition: The elements are simply placed on top of each other. Couplers: A coupler is applied around the elements and presses them together. Dowels and plates: A pin-like object penetrates the two elements. Notches: The elements are cut in a way so that they can be joined together and interlock.

***Does the connection allow for easy assembly, disassembly and reuse?***

The superposition and the notched connection have in this evaluation seemed easier to assemble, disassemble and reuse than the couplers and dowels. But this is highly dependent on the properties of each individual project. In any case though, the couplers and dowels demand some more time to apply since the elements cannot directly be put on each other. Along with the notched connection, they also generate a stiffness before complete assembly which the superposition connection does not.

***How is the appearance of the connection? Bulky or light?***

Since the connection is sort of integrated in the element for the superposition and notched connections, they can be considered to be lighter. But there are also possibilities to create highly integrated connections with couplers and dowels.

### ***What are the structural properties of the connection?***

Superposition: The connection creates a structure entirely based on the interlocking properties of a RF. Against horizontal forces the connection relies on friction between the elements. Couplers: Apart from the interlocking RF-effect, the couplers increase the friction between the elements by contraction. Dowels: The strength of the connection is dependent on the strength of the dowel, but also on the way it is embedded in the timber. Notches: Forces are transferred by geometrical blocking in the notch, creating surface compression.

## **9.3 Design/Analysis**

### ***What translational and rotational stiffness does the connection provide?***

Superposition (for a 45x45 mm<sup>2</sup> cross section):

$$Ct_x = 0 \text{ kN/m} \quad Ct_y = 0 \text{ kN/m} \quad Ct_z = 8325 \text{ kN/m}$$

$$Cr_x = 0 \text{ kNm/rad} \quad Cr_y = 0 \text{ kNm/rad} \quad Cr_z = 0 \text{ kNm/rad}$$

Notches (for a 45x45mm cross section, half lap joint):

$$Ct_x = 7448 \text{ kN/m} \quad Ct_y = 7448 \text{ kN/m} \quad Ct_z = 16650 \text{ kN/m}$$

$$Cr_x = 3.55 \text{ kNm/rad} \quad Cr_y = 3.55 \text{ kNm/rad} \quad Cr_z = 3.43 \text{ kNm/rad}$$

### ***How can a RF structure and the connections be modelled in a FEM software?***

In Karamba for Rhinoceros a short “column” can be inserted between the elements in the structure. The derived connection stiffness can then be inserted by using the Beam joint-component.

### ***How does the design of one connection type influence the structural behaviour of the overall structure, compared to another connection type?***

In this investigation, the superposition connection generated larger maximum deflection, bending moment and shear force in the structure compared to the notched connection. A half lap joint notch connection generated torsional moment in the beams which a superposition connection did not.

### ***What member sizes and connection detailing would be needed in a particular structural context with a certain span?***

To span a 5x5 meter span with a RF laid out in a certain “Leonardo-pattern”, carrying the structure’s self-weight and additional 130 kg applied as 2 kg weights in each connection, demanded a cross section of 45x95 mm timber C24. This was for using half lap joints with notches of half the height of the beams.

## **9.4 Physical model**

### ***How easy is assembly and disassembly?***

It was very easy to assemble and disassemble the physical model built for this thesis. One difficulty though, was to avoid breaking the fragile end part of each element where the notch was placed 42 mm from the edge. The end part tended to break when the structure was “lifted” to make room for assembly or disassembly of one element. There was also a risk of breaking it when transporting the beams or if a beam was accidentally dropped on the floor.

### ***Does the structural behaviour of the physical model match the FE model?***

When testing the physical model, the deflected structure looked similar to the one obtained in the FE model. Nevertheless, the magnitude of the deflection was much larger for the physical model compared to the FE model. For the SLS load the measured deflection was 30 mm while the FE model calculated 10 mm. The failure load was lower than calculated and happened in shear due to notch effect unlike the bending failure obtained in the FE model.

# 10 References

## 10.1 Literature

- Aicher, S., Garrecht, H., Reinhard, H.-W. (2014): *Materials and Joints in Timber Structures*. Springer, New York, pp. 129-134.
- Baverel, O. (2000): *Nexorades: a family of interwoven space structures*. Ph.D. Thesis. University of Surrey, Guildford
- Baverel, O., Popovic Larsen, O. (2011): A Review of woven Structures with Focus on Reciprocal Systems – Nexorades. *International Journal of Space Structures*, Vol. 26, No. 4, 2011, pp. 281-288.
- Dahlblom O, Olsson K-G (2010): *Strukturmekanik – Modellering och analys av ramar och fackverk (Structural Mechanics – Modelling and analysis of frames and trusses. In Swedish)*. Studentlitteratur AB, Lund.
- Descamps, T., Guerlement, G. (2009): Component method for the assessment of the axial, shear and rotational stiffness of connections in old timber frames. *9ième Congrès de Mécanique*, Marrakech, pp. 268-270.
- Garavaglia, E., Pizzigoni, A., Sgambi, L., Basso, N. (2013): Collapse behaviour in reciprocal frame structures. *Structural Engineering and Mechanics*, Vol. 46, No. 4, 2013, pp. 533-547.
- Gelez, S., Aubry, S., Vaudeville, B. (2011): Nexorade or Reciprocal Frame System Applied to the Design and Construction of a 850 m<sup>2</sup> Archaeological Shelter. *International Journal of Space Structures*, Vol. 26, No. 4, 2011, pp. 303-311.
- Gelez, S., Saby, V. (2011): Workshop « Ateliers Design » :« Nexorades, Facing an Emergency Situation ». *International Journal of Space Structures*, Vol. 26, No. 4, 2011, pp. 359-361.
- Jeska, S., Pascha, K.S. (2014): *Emergent Timber Technologies: Materials, Structures, Engineering, Projects*. Birkhäuser, Basel.
- Nateghi, F. (1995): Tests to determine the joint stiffness and resisting moment capacity of joints in timber-framed houses. *Journal of Engineering*, Vol. 8, No. 2, 1995, pp. 71-84.
- Pizzigoni, A. (2009): A High Fiber Reinforced Concrete Prototype for reciprocal structures of demountable building. *Proceedings of the International Association for Shell and Spatial Structures (IASS) Symposium*, Valencia, pp. 1895-1906.
- Popovic Larsen, O. (2008): *Reciprocal Frame Architecture*. Architectural press, Oxford.
- Popovic Larsen, O. (2014): Reciprocal Frame (RF) Structures: Real and Exploratory. *Nexus Network Journal*, Vol. 16, No. 1, 2014, pp. 119-134.
- Popovic Larsen, O., Lee, D., Lange, T. (2014): Sustainable Agricultural Building Design Using Locally Grown Danish Timber. *3rd International Workshop on Design in Civil and Environmental Engineering*, Kongens Lyngby, pp. 157-161.
- Porteous, J., Kermani, A. (2013): *Structural timber design to Eurocode 5*. Blackwell Publishing Ltd. Chichester.

- Pugnale, A., Sassone, M. (2014): Structural Reciprocity: Critical Overview and Promising Research/Design Issues. *Nexus Network Journal*, Vol. 16, No. 1, 2014, pp. 9-35.
- Pugnale, A., Parigi, D., Kirkegaard, P.H., Sassone, M. (2011): *The Principle of Structural Reciprocity*. Hemming Group Ltd. London.
- Rizzuto, J.P., Popovic Larsen, O. (2010): Connection Systems in Reciprocal Frames and Mutually Supported Elements in Space Structure Networks. *International Journal of Space Structures*, Vol. 25, No. 4, 2010, pp. 243-256.
- Shiratori, T., Komatsu, K., Leijten, A. (2008): Modified traditional Japanese timber joint system with retrofitting abilities. *Structural Control and Health Monitoring*, Vol 15, No. 7, 2008, pp. 1036-1056.
- Swedish Wood (2011): *Design of timber structures*, Swedish Forest Industries Federation, Stockholm.
- Thönnissen, U. (2014): A Form-Finding Instrument for Reciprocal Structures. *Nexus Network Journal*, Vol. 16, No. 1, 2014, pp. 89-107.
- Thönnissen, U. (2015): *Hebelstabwerke / Reciprocal Frameworks: Tradition and Innovation*. gta Verlag, Zürich.

## 10.2 Web

- Spiro, A., 2012, *Hebelstabwerke*. Available from:  
<http://www.spiro.arch.ethz.ch/de/research/reciprocal-frame.html> (Accessed 2016-03-14).
- That Roundhouse, n.d., *Making a Reciprocal frame roof*. Available from:  
[www.thatroundhouse.info](http://www.thatroundhouse.info) (Accessed 2016-03-14).

## 10.3 Images

- [1] Figure 2.1: “Indian tepee and Hogan dwelling. (Sketch by A.E. Piroozfar.)”, Popovic Larsen, O. (2008). Reciprocal Frame Architecture. Architectural press, Oxford, pp. 6.
- [2] Figure 2.2: “Honnecourt’s planar grillage assembly. (Sketch by A.E. Piroozfar.)”, Popovic Larsen, O. (2008). Reciprocal Frame Architecture. Architectural press, Oxford, pp. 8.
- [3] Figure 2.3: “Leonardo da Vinci’s proposals for temporary bridges. (Sketch by A.E. Piroozfar.)”, Popovic Larsen, O. (2008). Reciprocal Frame Architecture. Architectural press, Oxford, pp. 11.
- [4] Figure 2.5: “Auditorium – internal view of the oppressive space. (Photo: Kazuhiko Ishii.)”, Popovic Larsen, O. (2008). Reciprocal Frame Architecture. Architectural press, Oxford, pp. 101.
- [5] Figure 2.6: “organic architecture” by INCITE researchers, Licensed under Creative Commons Attribution CC BY-SA 2.0,  
<https://www.flickr.com/photos/incite/22329862/> (Accessed 2016-04-06).

[6] Figure 2.7: Photo © Bibracte-Antoine Maillier, Drawing © Paul Andreu,  
<http://www.bibracte.fr/fr/approfondir/les-coulisses-de-bibracte/la-gestion-dun-site-dexception/un-abri-innovant-pour-la-protection-des-vestiges> (Accessed 2016-04-13).

[7] Figure 2.8: “*Reciprocal frame structure*” by Lorenz Lachauer, Licensed under Creative Commons Attribution CC BY-NC-SA 2.0,  
<https://www.flickr.com/photos/79880145@N03/8546162818/> (Accessed 2016-04-06).

[8] Figure 4.3: Pizzigoni, A. (2016) Email to Joel Gustafsson, 4 April.

[9] Figure 4.6: Wrench, T. (2016) Email to Joel Gustafsson, 15 March.

[10] Figure 4.7: Wrench, T. (2016) Email to Joel Gustafsson, 15 March.

[11] Figure 4.10: “*Chun Qing Li's Sustainable Wooden Kreod Pavilion*” by Inhabitat, Licensed under Creative Commons Attribution CC BY-NC-ND 2.0,  
<https://www.flickr.com/photos/inhabitat/8032321256/> (Accessed 2016-04-06).

[12] Figure 4.11: “*Chun Qing Li's Sustainable Wooden Kreod Pavilion*” by Inhabitat, Licensed under Creative Commons Attribution CC BY-NC-ND 2.0,  
<https://www.flickr.com/photos/inhabitat/8032322787/> (Accessed 2016-04-06).

[13] Figure 4.14: “*The double height space of the exhibition hall makes the space feel bigger than it really is. (Photo: Kazuhiro Ishii.)*”, Popovic Larsen, O. (2008). Reciprocal Frame Architecture. Architectural press, Oxford, pp. 93.

[14] Figure 4.15: “*Assembling the pre-cut RF timber beams. (Photo: Kazuhiro Ishii.)*”, Popovic Larsen, O. (2008). Reciprocal Frame Architecture. Architectural press, Oxford, pp. 96.